AD-A064 430 WRIGHT STATE UNIV DAYTON OHIO F/G 21/2
IN-SITU MEASUREMENTS OF GAS SPECIES CONCENTRATIONS.(U)
AUG 78 C CHANG, G D SIDES, T O TIERNAN F33615-76-C-2010
UNCLASSIFIED AFAPL-TR-78-64 NL

1 OF 1
AD A064430

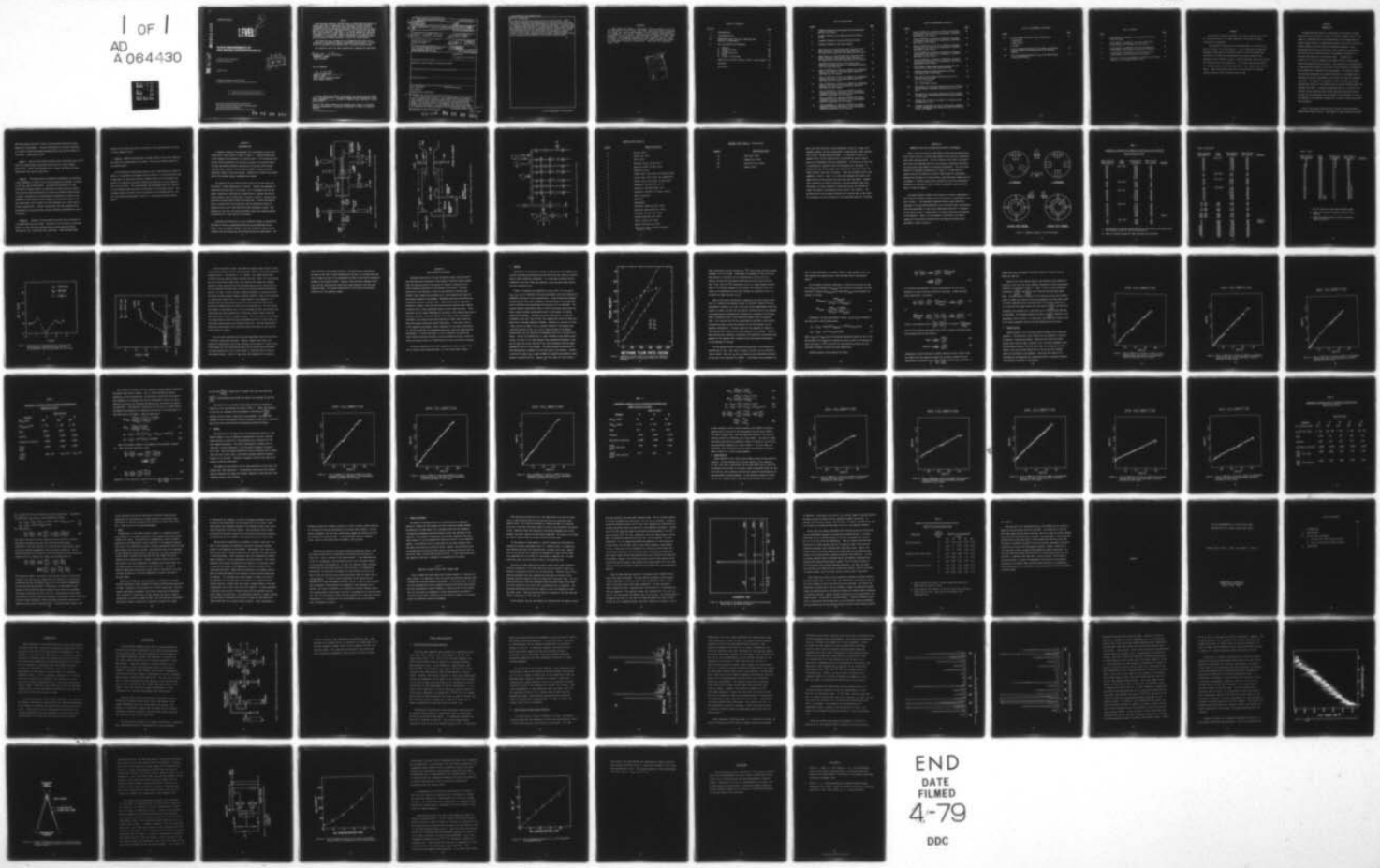

END
DATE FILMED
4-79
DDC

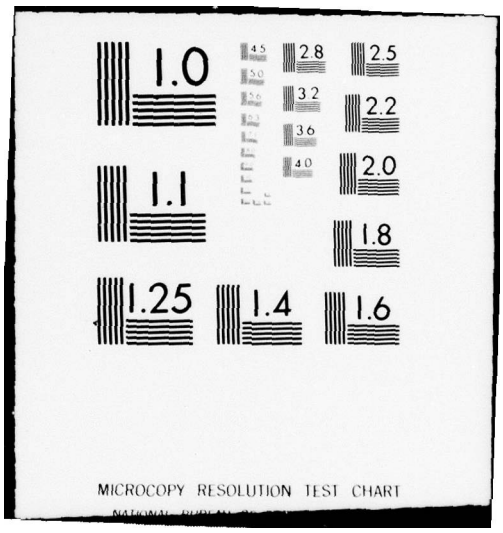
1.0
1.1
1.25
1.4
1.6
1.8
2.0
2.2
2.5
2.8
3.2
3.6
4.0
4.5
5.0
5.6
MICROCOPY RESOLUTION TEST CHART

AFAPL-TR-78-64

LEVEL II

AD A064430

DDC FILE COPY

IN-SITU MEASUREMENTS OF GAS SPECIES CONCENTRATIONS (U)

WRIGHT STATE UNIVERSITY
DAYTON, OHIO 45435

AUGUST 1978

TECHNICAL REPORT AFAPL-TR-78-64
Final Report for Period 15 November 1976 to 15 June 1978

Approved for public release; distribution unlimited.

AIR FORCE AERO PROPULSION LABORATORY
AIR FORCE WRIGHT AERONAUTICAL LABORATORIES
AIR FORCE SYSTEMS COMMAND
WRIGHT-PATTERSON AIR FORCE BASE, OHIO 45433

NOTICE

When Government drawings, specifications, or other data are used for any purpose other than in connection with a definitely related Government procurement operation, the United States Government thereby incurs no responsibility nor any obligation whatsoever; and the fact that the government may have formulated, furnished, or in any way supplied the said drawings, specifications, or other data, is not to be regarded by implication or otherwise as in any manner licensing the holder or any other person or corporation, or conveying any rights or permission to manufacture, use, or sell any patented invention that may in any way be related thereto.

This report has been reviewed by the Information Office (OI) and is releasable to the National Technical Information Service (NTIS). At NTIS, it will be available to the general public, including foreign nations.

This technical report has been reviewed and is approved for publication.

Raghunath S Boray

RAGHUNATH S. BORAY
Project Engineer

FOR THE COMMANDER

Frank D Stull

FRANK D. STULL
Chief, Ramjet Technology Branch
Ramjet Engine Division

"If your address has changed, if you wish to be removed from our mailing list, or if the addressee is no longer employed by your organization please notify AFAPL/RJT, W-PAFB, OH 45433 to help us maintain a current mailing list."

Copies of this report should not be returned unelss return is required by security considerations, contractual obligations, or notice on a specific document.

AIR FORCE/56780/16 January 1979 — 130

SECURITY CLASSIFICATION OF THIS PAGE *(When Data Entered)*

REPORT DOCUMENTATION PAGE

READ INSTRUCTIONS BEFORE COMPLETING FORM

1. REPORT NUMBER: AFAPL-TR-78-64	2. GOVT ACCESSION NO.
3. RECIPIENT'S CATALOG NUMBER	
4. TITLE *(and Subtitle)*: IN-SITU MEASUREMENTS OF GAS SPECIES CONCENTRATIONS	5. TYPE OF REPORT & PERIOD COVERED: Final Technical Report, 15 Nov 76 — 15 Jun 78
	6. PERFORMING ORG. REPORT NUMBER
7. AUTHOR(s): C. Chang, G. D. Sides, T. O. Tiernan	8. CONTRACT OR GRANT NUMBER(s): F33615-76-C-2018
9. PERFORMING ORGANIZATION NAME AND ADDRESS: Wright State University, Dayton, OH 45435	10. PROGRAM ELEMENT, PROJECT, TASK AREA & WORK UNIT NUMBERS: 2308-S2-26 S2
11. CONTROLLING OFFICE NAME AND ADDRESS: Air Force Wright Aeronautical Laboratories, Air Force Aero Propulsion Laboratory, Ramjet Technology Branch /RJT, Wright-Patterson AFB, OH 45433	12. REPORT DATE: Aug 78
	13. NUMBER OF PAGES: 91 p.
14. MONITORING AGENCY NAME & ADDRESS *(if different from Controlling Office)*	15. SECURITY CLASS. *(of this report)*: UNCLASSIFIED
	15a. DECLASSIFICATION/DOWNGRADING SCHEDULE

16. DISTRIBUTION STATEMENT *(of this Report)*

Approved for public release, distribution unlimited.

17. DISTRIBUTION STATEMENT *(of the abstract entered in Block 20, if different from Report)*

18. SUPPLEMENTARY NOTES

19. KEY WORDS *(Continue on reverse side if necessary and identify by block number)*

Mass Spectrometry
Species Concentrations
Gas Sampling
Quadrupole Mass Spectrometer

20. ABSTRACT *(Continue on reverse side if necessary and identify by block number)*

(U) This report gives the results of in-situ measurements of the concentrations of a simulated fuel (argon) in a dump combustor flow field, obtained using a sampling probe - mass spectrometer system. These data demonstrate the improved fuel-air mixing which is realized by utilizing specialized flame holders. The existence of swirl in the combustor flow field has also been established by these studies. The work described herein required more elaborate interfacing of the mass spectrometer with a gas calibration system which

(Continued on Reverse Side)

DD FORM 1 JAN 73 1473 EDITION OF 1 NOV 65 IS OBSOLETE

Block No. 20 Continued:

was designed, fabricated and tested during this reporting period. Several preliminary experiments were conducted using this gas calibration system, for the purpose of devising suitable methodology for detecting specific gas species of interest in connection with future combustion experiments. Calibration data and coefficients were obtained for the gases, methane, carbon dioxide and oxygen, and calibration data for water and carbon monoxide is presently being obtained. Some preliminary work was also accomplished in monitoring nitric oxide at the parts-per-million level, using the existing mass spectrometric diagnostic system. Finally, several experiments were conducted in sampling gaseous species from a Bunsen burner flame employing various types of sampling probes.

FOREWORD

This report describes a contractual research effort involving the operation of an on-line, real-time, mass spectrometric monitoring system for in-situ measurements of gas species concentrations in a combustor flow field. The work was performed by Wright State University, under contract F33615-76-2010 in support of Work Unit 2308S226. The technical monitor for this contract was Dr. James E. Drewry of the Ramjet Engine Division, Ramjet Technology Branch, Air Force Aero Propulsion Laboratory. This work was completed August 1978.

TABLE OF CONTENTS

LIST OF ILLUSTRATIONS

LIST OF ILLUSTRATIONS (continued)

LIST OF ILLUSTRATIONS (continued)

LIST OF TABLES

SUMMARY

During this reporting period, the in-situ monitoring of Ar/air mixing profiles in a dump combustor flow field has been successfully completed.

Considerable progress has also been made in achieving the goals of Phase II of the project. A gas calibration system was designed, fabricated, and demonstrated to function adequately. Preliminary calibration experiments have been conducted for methane, carbon dioxide, oxygen, carbon monoxide, water and oxides of nitrogen using this apparatus. This work provides the basis for future studies involving sampling of real combustion environments. Some preliminary work was also conducted in sampling gaseous species from a Bunsen burner flame.

SECTION I

INTRODUCTION

The work described herein is a continuation of previously initiated research which was discussed in detail in an earlier summary report.[1] This research is concerned with in-situ measurements of the concentrations of various gaseous species in simulated dump combustor flow fields, utilizing a facility located at the Air Force Aero Propulsion Laboratory. Work accomplished during the period covered by this report has concentrated on the installation and characterization of a diagnostic system which is directly interfaced with a 30-inch wind tunnel. Simulated fuel as well as air, from this combustor were sampled using a sampling probe which was inserted into the flow field. Data relating to the concentrations of these gases are acquired in real-time via the diagnostic instrumentation, which incorporates a quadrupole mass spectrometer. Ion intensity signals from the mass spectrometer are transmitted directly to a computer which is interfaced to the mass spectrometer, and the data is stored for subsequent processing. The computer is programmed to reduce this data and produce concentration profiles of the simulated fuel at various locations within the combustor flow field. In studies accomplished thus far, a series of such profiles have been obtained under various operating conditions which are critical for the determination of the fuel/air mixing mechanism, as well as for modeling of the combustor configuration, in order to improve the combustion efficiency.

Early in the present reporting period, several planning meetings of Wright State personnel with Dr. James Drewry and other personnel associated

with this project were held in order to more precisely define the current objectives of the program. The near-term objectives which were identified as a result of these discussions were appropriately cast into four phases of the project. These were as follows:

Phase I. The cold flow testing initiated during the previous year of this effort was to be continued, using the existing facility, without further modification. Several newly designed (by Dr. Drewry) and fabricated flame holders were to be used for these tests.

Phase II. This phase entails development of methodology for monitoring several compounds of interest in the active combustion environment, including O_2, CO, CO_2, H_2O and hydrocarbons. The design and fabrication of a gas calibration system was required in connection with these monitoring studies. This work also required preparation of various gas standard mixtures having a range of concentrations, the development of procedures for detecting the components of each standard mixture prepared, and the determination of the mass spectrometer signal response for these components over a wide range of mixture concentrations. Possible interferences from other compounds which were expected to be present during a typical combustion experiment were also to be assessed.

Phase III. Testing of the gas monitoring system using a burner was to be accomplished during this phase. The burner to be utilized was a flat-flame burner, for which the flame characteristics and the combustion product distributions had already been well established. These experiments were

expected to yield test data useful in the design of the sampling probe to be used in future combustion tests.

Phase IV. Sampling and monitoring of gaseous products from actual combustion tests were to be accomplished in this phase. This was the ultimate objective of the present project.

At the conclusion of the present contract, most of the objectives planned for Phases I, II and some of the planned efforts for Phase III of the program have been accomplished, but significant technical problems remain to be solved before the objective of applying the diagnostic methods described here to actual combustion tests can be realized. The accomplishments and achievements under this contract for the indicated reporting period are described in the following sections. Work completed during the initial year of the contract is not presented herein, since this has already been discussed in detail in a previously published Technical Report.[1]

SECTION II

INSTRUMENTATION

A schematic diagram of the quadrupole mass spectrometer and gas inlet system used in these studies is shown in Figure 1. A detailed description of this apparatus was presented in a previous report.[1] This system was used without further modification for the work discussed in the present report. The mass spectrometer operated satisfactorily during this entire period, requiring minor cleaning of the ion source assembly to reduce excessive background signals on only one occasion. Cleaning of the source, and replacement of the filament largely eliminated this problem.

The combustor and gas sampling system, which has also been described previously[1] is shown schematically in Figure 2. Briefly, the procedure for conducting cold-flow tests is as follows. Air is introduced into the combustor, along with a simulated fuel (argon) which is injected into the air stream through a total of eight ports, as shown in Figure 2. Mixing of the argon and air occurs mainly within the mixing zone. A traversing sampling probe is placed within this mixing zone, and the sampled gas mixture is analyzed on-line, and in real-time by the mass spectrometer system. Data obtained for such cold flow mixing experiments during this reporting period are described in a later section of the report.

The design and fabrication of a gas calibration system, as specified by the Phase II plan was accomplished during the present reporting period. Figure 3 gives a schematic diagram of this gas calibration system, and the interface with the existing gas inlet system and the mass spectrometer. The

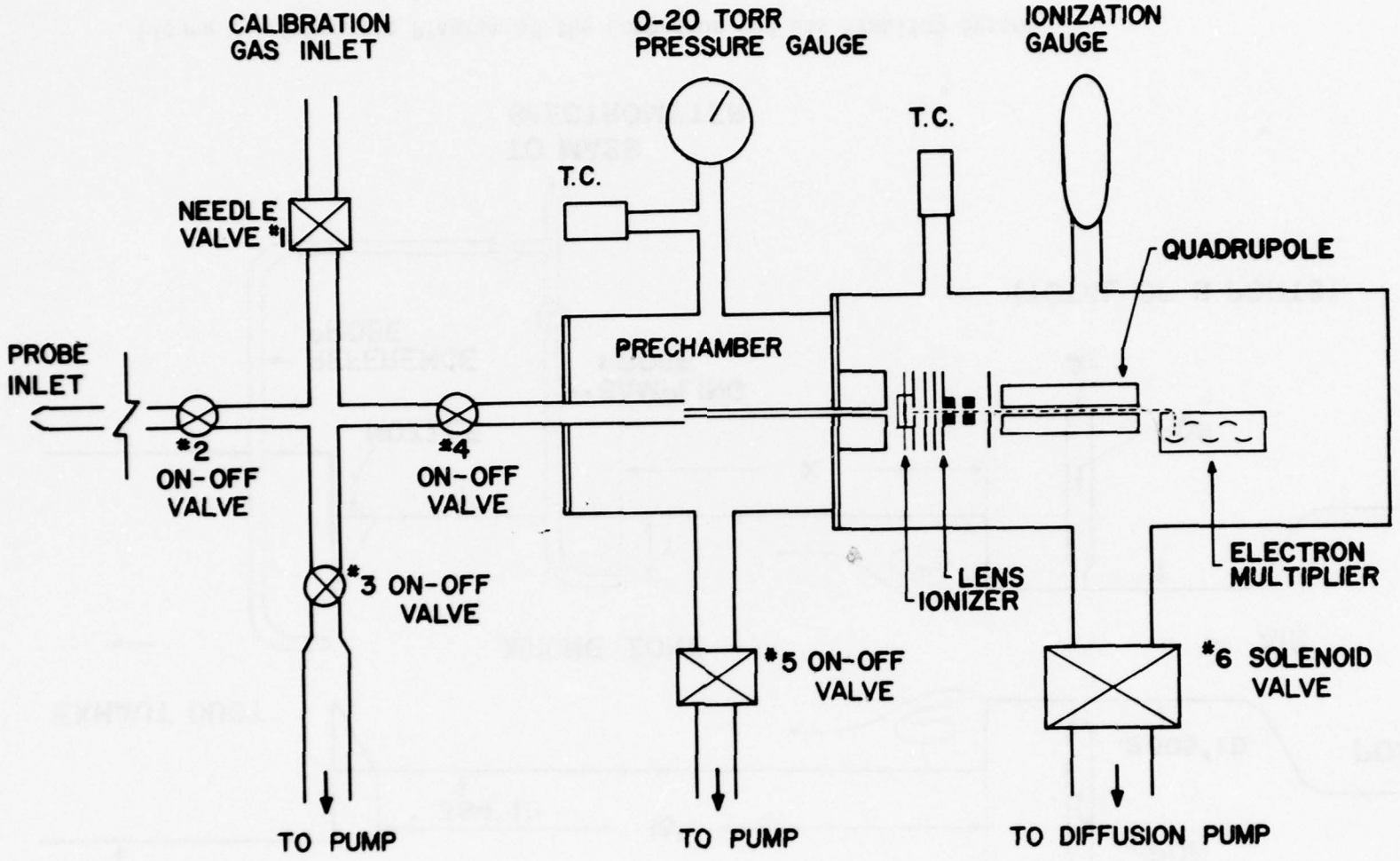

Figure 1. Schematic Diagram of the Quadrupole Mass Spectrometer and Gas Inlet System

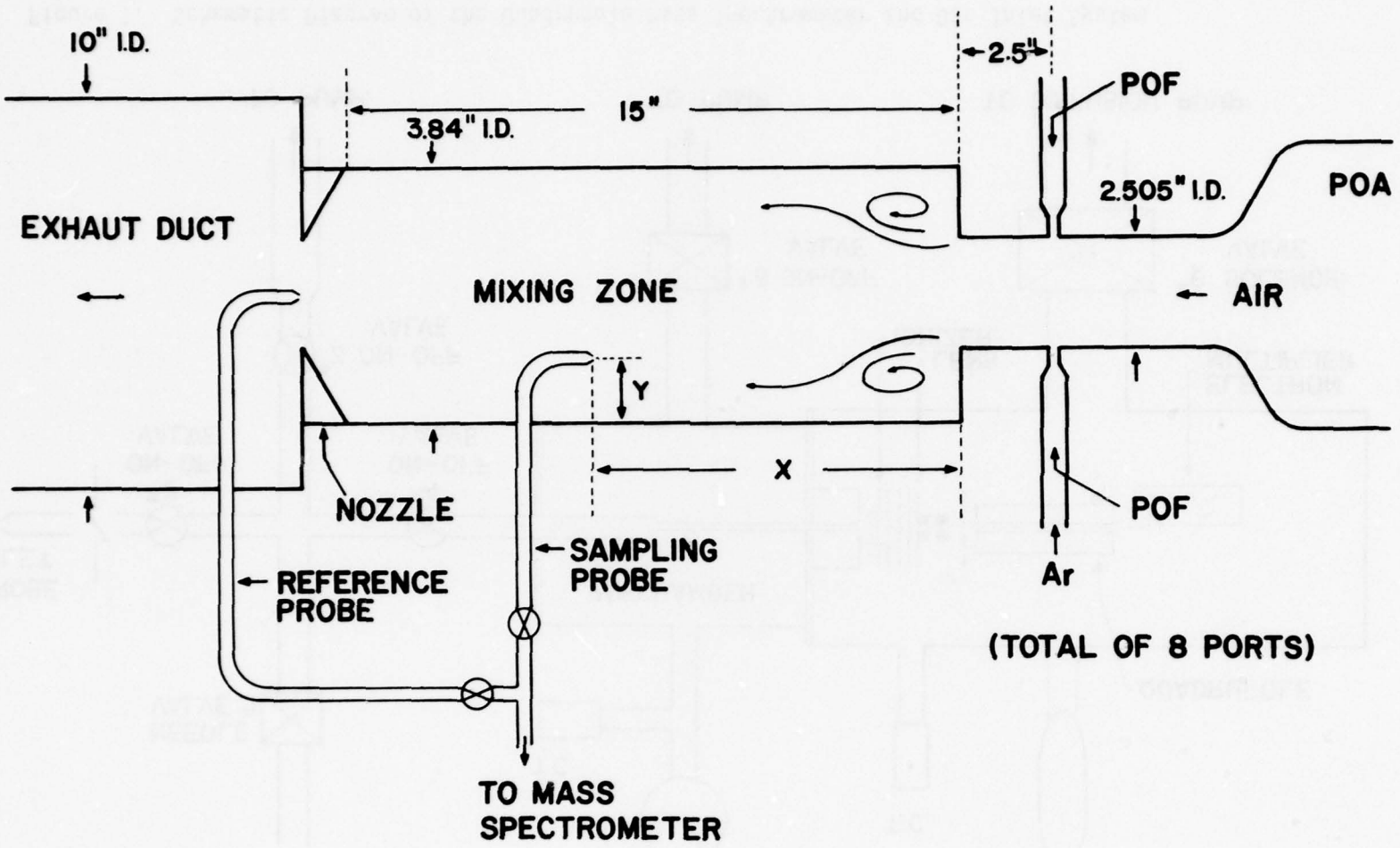

Figure 2. Schematic Diagram of the Combustor and Gas Sampling System

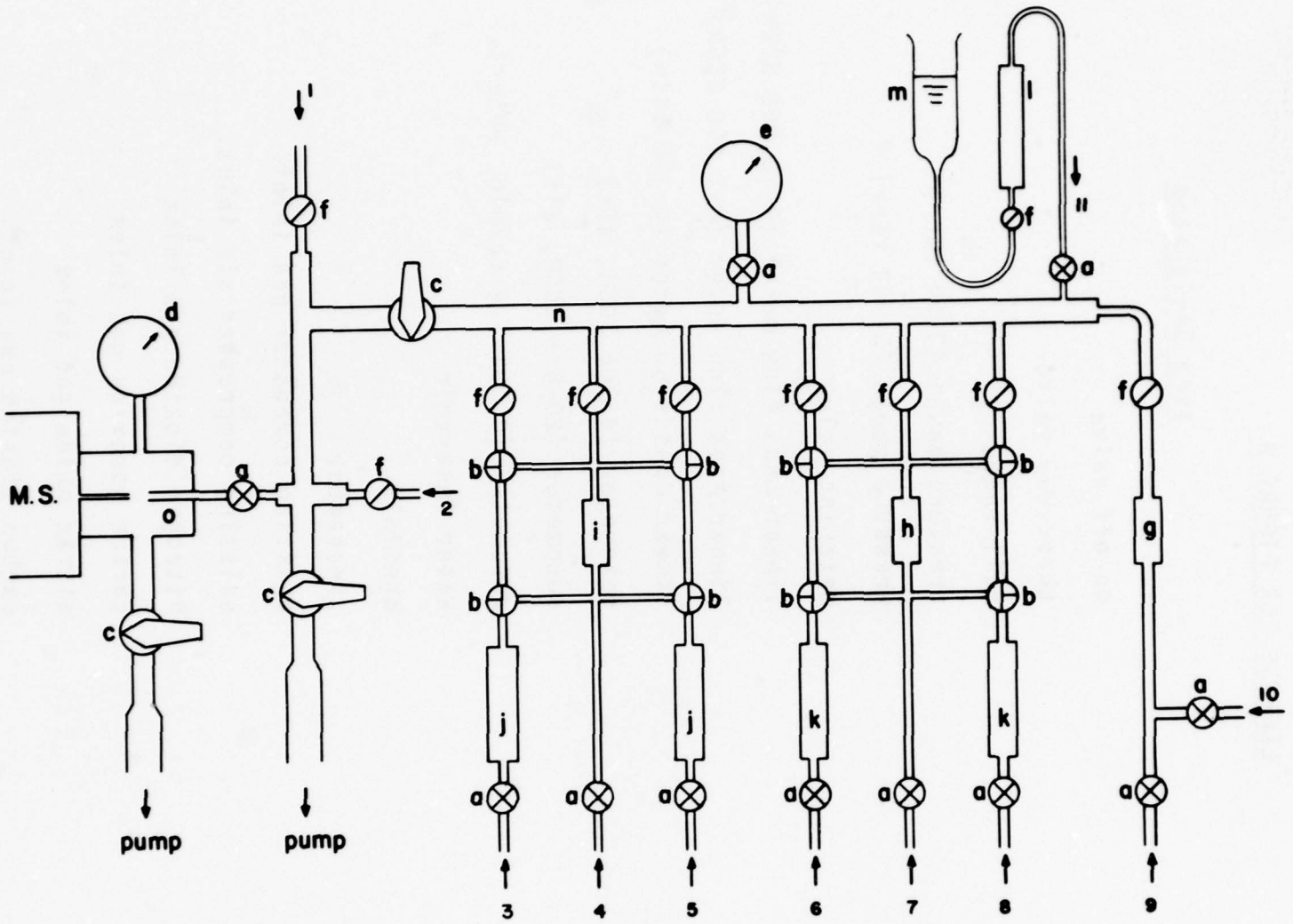

Figure 3. Schematic Diagrams of the Gas Calibrations Systems

LEGENDS FOR FIGURE 3

Legend	Item Designated
a	on-off valve
b	three-way valve
c	ball valve
d	pressure gauge (0-50 torr)
e	pressure gauge (0-300 torr)
f	metering valve
g	linear mass flow meter (0-10,000 SCCM)
h	linear mass flow meter (0-1,000 SCCM)
i	linear mass flow meter (0-100 SCCM)
j	rotometer (4-166 SCCM, air)
k	rotometer (20-859 SCCM, air)
l	rotometer (0.003-1.4 cc/min, water)
m	water reservoir
n	manifold
o	prechamber
1.	existing combustor gas inlet.
2.	existing compressed air inlet.
3.	nitrogen dioxide gas inlet
4.	carbon monoxide gas inlet
5.	nitric oxide gas inlet
6.	carbon dioxide gas inlet
7.	fuel and carbon dioxide standard mixture inlet

LEGENDS FOR FIGURE 3 (Continued)

Legend	Item Designated
8.	fuel gas inlet
9.	oxygen gas inlet
10.	auxiliary gas inlet
11.	water inlet

gases which were monitored in these experiments include air, oxygen, fuel (methane, propane, and other hydrocarbons), carbon dioxide, carbon monoxide, nitric oxide, nitrogen dioxide and water. As indicated in Figure 3, a separate inlet line and injection port are provided for each of several gases to be introduced to the mass spectrometer. The flow rate in each line is controlled by a metering valve (f) and measured by a flow meter. To minimize the cost of this system, only three of the lines were fitted with highly accurate linear mass flow meters. These were installed in the lines numbered 4, 7 and 9. Lines 3, 5, 6 and 8 were equipped with regular rotometers which are less accurate than the linear mass flow meters. However, these rotometers are readily calibrated, using the adjacent linear mass flow meters, by simply temporarily redirecting the gas flow through the linear flow meters, using three-way valves shown in the schematic. The gas manifold can also be readily heated using a heating tape, as was found to be necessary for the calibration of the system when water was introduced.

SECTION III

COMBUSTOR FLOW FIELD GAS SAMPLING AND ANALYSIS EXPERIMENTS

Table I lists the results of experiments in which in-situ monitoring of Ar/air mixing profiles in the APL dump combustor flow field was accomplished during this reporting period. The first section of this table lists experiments which were conducted mainly for the purpose of evaluating the effects of using various flame holders of different configuration. Four such flame holders are illustrated schematically in Figure 4. As described in a separate report,[2] the addition of certain flame holders has considerably improved the efficiency of air/fuel mixing, which effectively reduces the L/D requirement. A typical mixing profile obtained for one set of experimental conditions (as indicated in Table 1) using the diagnostic system described above, is shown in Figure 5.

The second section of Table I lists data for a series of experiments in which argon was injected through only one or two ports, as specified for each test in Table 1. This new mode of operation permits a more definitive assessment of the gas mixing mechanism in the flow fields under investigation. From these experiments, it was clearly demonstrated that swirl is important in the mixing process, a finding which is of major significance for modeling of the combustor. Again, for the purposes of illustration, one typical example of a mixing profile obtained with the operating conditions just described is shown in Figure 6.

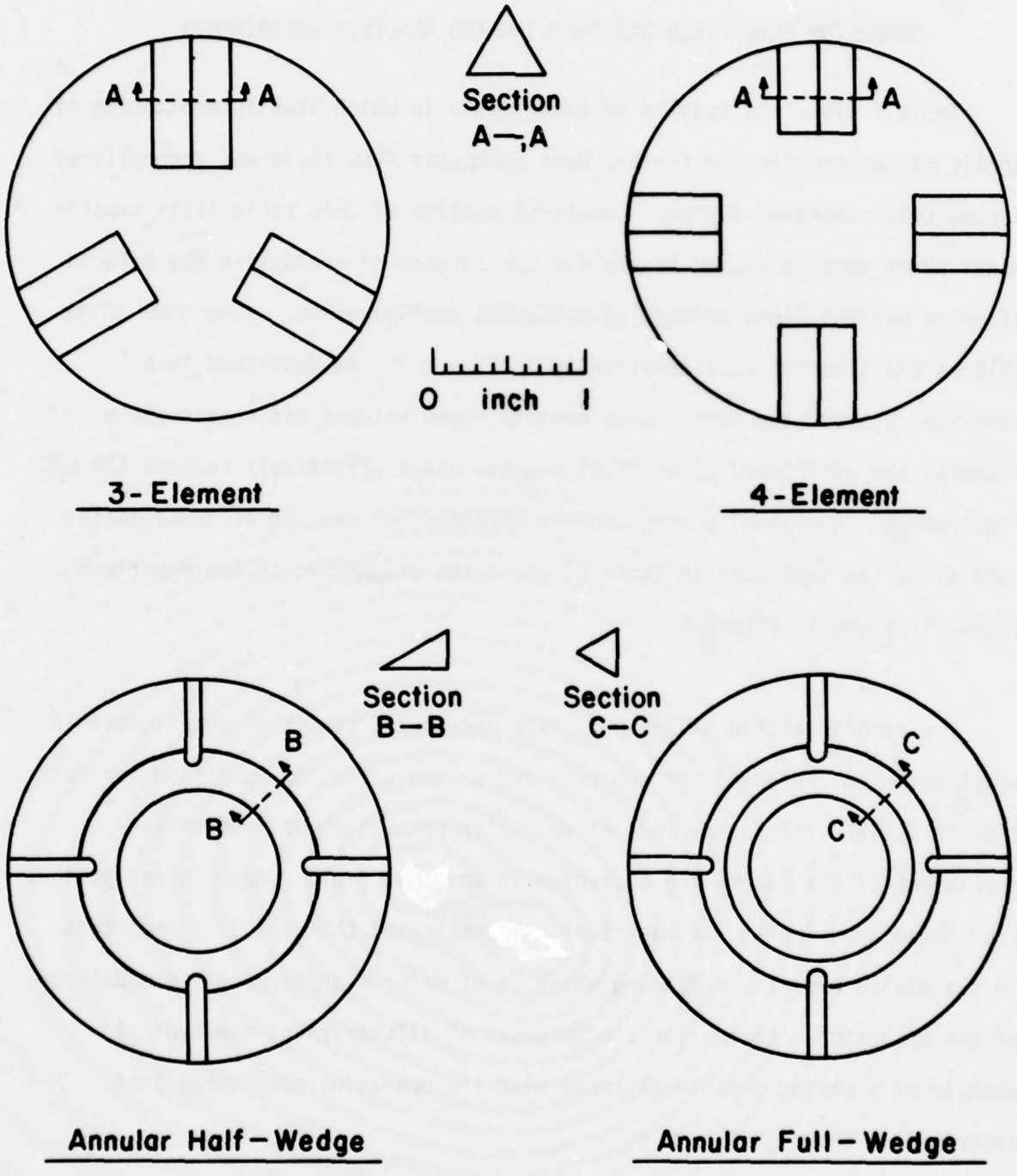

Figure 4. Schematic Diagrams of the Flame Holders

TABLE 1.

EXPERIMENTAL PARAMETERS FOR ARGON/AIR MIXING PROFILE TESTS COMPLETED DURING REPORTING PERIOD

Argon Injection port position[a]	Flame Holder	Probe Position x (inches)	Argon Pressure P_{of} (psia)	Reference
all[b]	HW-1 (90°)	8.69	89	
all		8.69	129	
all		2.69	129	
all		2.69	89	
all		5.43	89	
all		5.43	129	
all		11.43	129	
all		11.43	89	
all	HW-1 (45°)	11.43	89	
all		5.43	89	
all		2.69	89	
all		2.69	129	
all	HW-1 (0°)	2.69	130	
all		2.69	89	
all		8.69	89	
all		11.43	89	
all		11.43	129	
all		5.43	129	
all		5.43	89	
all	HW-2 (o°)	5.43	89	
all		5.43	129	
all		11.43	129	
all		11.43	89	
all		8.69	89	
all		8.69	129	
all		2.69	129	
all		2.69	89	Figure 5
all	HW-2 (45°)	2.69	89	
all		2.69	129	
all		2.69	89	

a. The positions of the argon injection parts are indicated by their phase angles with reference to that of the top injection port.

b. Argon is injected through all eight injection ports available.

Table 1. (Continued)

Argon Injection port position	Flame Holder	Probe Position x (inches)	Argon Pressure P_{of} (psia)	Reference
all	HW-2 (0°)	8.69	89	
all		8.69	129	
all		2.69	129	
all		2.69	89	
all		5.44	89	
all		5.44	129	
all		11.44	129	
all		11.44	89	
all	FW-2 (45°)	2.69	89	
all		2.69	129	
all	FW-1 (0°)	2.69	129	
all		8.69	129	
all		11.44	129	
all		5.44	129	
all	3-EL-(90°)	5.44	129	
all		5.44	89	
all		11.44	89	
all		11.44	129	
all		8.69	129	
all		8.69	89	
all		2.69	89	
all		2.69	129	
0°; 180°	none	2.69	129	
0°; 180°	none	8.69	129	
0°; 180°	none	11.44	129	
0°; 180°	none	5.44	129	
90°; 270°	none	5.44	129	
90°; 270°	none	2.69	129	
90°; 270°	none	8.69	129	
0°	none	8.69	204	Figure 6
0°	none	2.69	202	Figure 6
0°	none	2.69	130	
180°	none	2.69	129	
180°	none	2.69	204	
180°	none	8.69	203	
180°	none	8.69	129	
180°	none	11.44	129	
180°	none	11.44	203	
0°	none	11.44	203	

Table 1. (Cont.)

Argon Injection Port Position	Flame Holder	Probe Position x (inches)	Argon Pressure of (psia)	Reference
0°	none	11.44	129	
0°	none	5.44	203	
0°	none	5.44	129	
180°	none	5.44	203	
180°	none	5.44	129	
all	none	0.1	129	
all	none	0.1	129	
all	none	0.1	129	
all	none	0.1	90	
all	none	0.1	45	
all	none	0.1	129	
all	none	0.1	90	
all	none	0.1	45	
all	none	0.1	90[c]	
all	none	0.1	129[c]	
all	none	0.1	45[c]	
all	none	0.1	90[c,d]	
all	none	0.1	129[c,d]	
all	none	0.1	129[c,e]	
all	none	0.1	45[c,d]	
all	none	0.1	45[c,e]	
all	FW-1 (0°)	0.1	90[c,d]	
all	FW-1 (0°)	0.1	45[c,d]	
all	FW-1 (0°)	0.1	129[c,d]	

c. Date are acquired at high speed integration mode.

d. Probes are traversed at opposite direction during sampling.

e. Probes are manually moved to several preselected sampling positions.

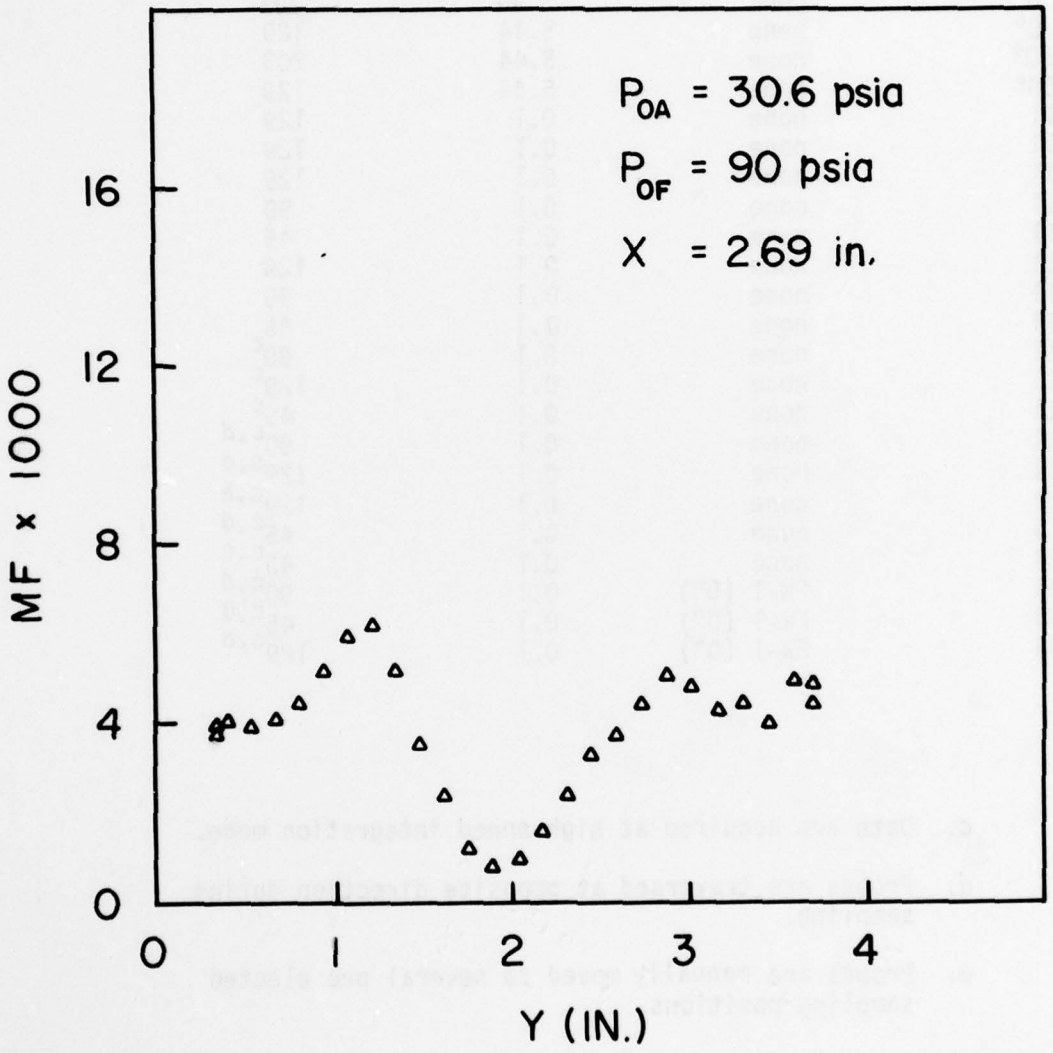

Figure 5. Mole Fraction of Injected Argon As a Function of the Radial Position of the Sampling Probe (See Table I for experimental conditions applicable to this figure)

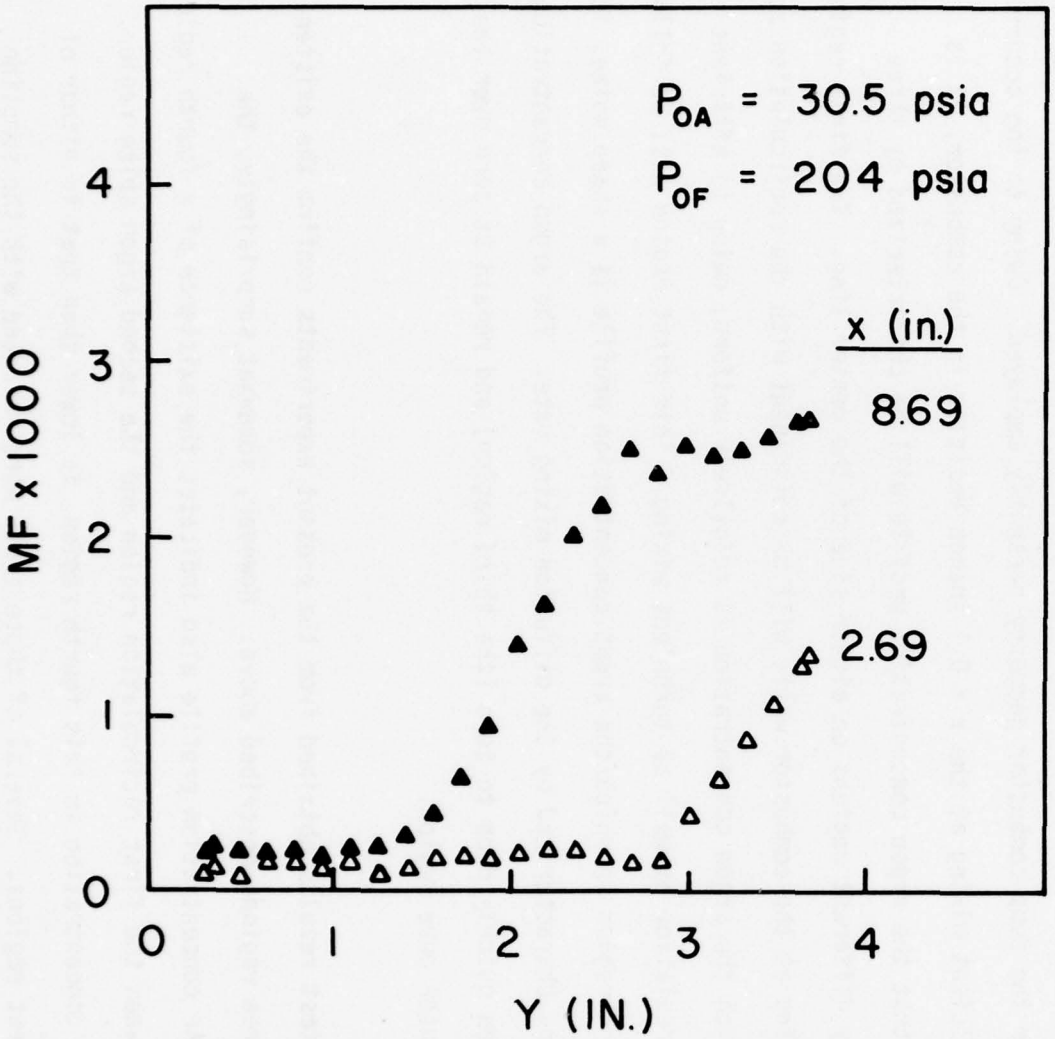

Figure 6. Mole Fraction of Injected Argon As a Function of the Radial Position of the Sampling Probe (See Table I for experimental conditions applicable to this figure)

In the last section of Table 1 are shown for another series of tests in which a new sampling probe was used for sampling gaseous species in the region immediately following the air inlet section (x = 0.1 inches). This region had not been accessible with the sampling probes previously utilized. Static air inlet pressure was set at 30.5 psia for these tests, and simulated fuel (argon) was injected through all eight injection ports with upstream pressures of 45, 90 and 129 psia. The data obtained from these tests, along with previously measured concentration profiles at larger x values, provide a complete assessment of unreactive air/fuel mixing for the dump combustor geometry presently employed. Owing to the occurrence of insufficient mixing at the x = 0.1 inches position in the combustor, it is expected that the argon concentration profile will be characterized by three distinctly different regions on either side of the center line. The first region, which begins at the combustor wall, will be coincident with the recirculation zone, within which the argon concentration is relatively uniform, owing to efficient eddy recirculation as well as turbulent mixing. This first region will be followed by a second region in which the argon concentration profile is a sharp spike, its width being characterized by the diffusion mixing rate. The argon concentration should then quickly drop to zero (the third region) and remain at zero over the entire center core region.

The test results obtained from the present experiments confirm the existence of the three regions described above. However, somewhat surprisingly, the observed Ar concentration profile also indicates the existence of a fourth region, lying between the first recirculation region and the second argon spike region. The argon concentration in this fourth region is lower than that in either of the adjacent regions. Several of these tests were repeated with the sampling

probe traversing in the reverse direction. The results again confirmed the existence of the "dip" in argon concentration, and thus it is unlikely that this drop is simply the result of an experimental artifact arising from the mechanical movement of the traversing probe. Recently, these tests were repeated a third time, with the interfaced data acquisition system operated in the high speed integration mode. This permits determination of the detailed concentration profiles of all the combustor regions.

SECTION IV

GAS CALIBRATION EXPERIMENTS

Following construction of the gas calibration system, several preliminary experiments were conducted for the purpose of devising suitable methodology for detecting specific gas species of interest in connection with actual combustion experiments to be conducted in the future. Detection sensitivity of the apparatus, as well as the linearity of the mass spectrometer signal response were examined over a large concentration range for each gaseous compound to be measured. Calibration data and coefficients were subsequently obtained in several cases. These results must be regarded as preliminary, however, since true calibrations must be obtained under sampling conditions which closely approximate those of actual combustion tests. These conditions will be largely determined by the design of the sampling probe used in the tests, and this is not well defined at this stage of the investigation. Furthermore, the present results were obtained only under ideal conditions, where each gaseous species was tested individually. In the actual tests of a real combustion environment, several compounds will be present simultaneously, and the possibility of interferences may arise, which will complicate the measurements. In future experiments, it will be necessary to develop more sophisticated calibration procedures, using multicomponent mixtures, which will permit the possible effects of interferences to be more realistically evaluated.

Calibration experiments which were accomplished to date, for each of the several gaseous species mentioned above, will now be described in detail.

1. Methane.

Calibration of the analytical system for methane was first attempted during this reporting period because this gas will be the fuel which is initially used in actual combustion experiments. It is desirable to monitor the distribution of this fuel inside the combustor, since such data yields directly the fuel consumption rate.

Figure 7 illustrates the intensities of ions at m/e = 14, 15, and 16 (I_{14}, I_{15}, I_{16}) as indicated by the mass spectrometer, which were obtained for methane/air mixtures of various concentrations. These mixtures were prepared by adjusting the flow rates of methane to selected values in the range from zero to 200 SCCM, while maintaining the flow rate of air at 2000 SCCM. This range of methane concentration (from 0 to 9% of the mixture) should span the actual range of methane concentrations which is anticipated in a typical combustion environment. The three ion masses cited (m/e 14, 15, and 16) correspond to the CH_2^+, CH_3^+ and CH_4^+ ions respectively, which are three well-known ions in the mass spectrum of methane. Obviously, as the data in Figure 7 show, the m/e 14 signal is not a suitable indicator of the methane level since the intensity of this ion is not a linear function of the methane concentration, and its relatively low abundance results in a low sensitivity factor. The m/e 16 intensity also is a poor indicator of the methane concentration (in spite of its linear behavior with concentration) because a large m/e 16 signal also arises from the O^+ ion, which originates from the oxygen component of the air in the mixture. This would preclude the monitoring of low concentrations of methane if m/e 16 were used as the indicator. Obviously the m/e 15 signal (I_{15}) is most reliable for monitoring the methane concentration in mixtures with air. However, this ion signal will also include a

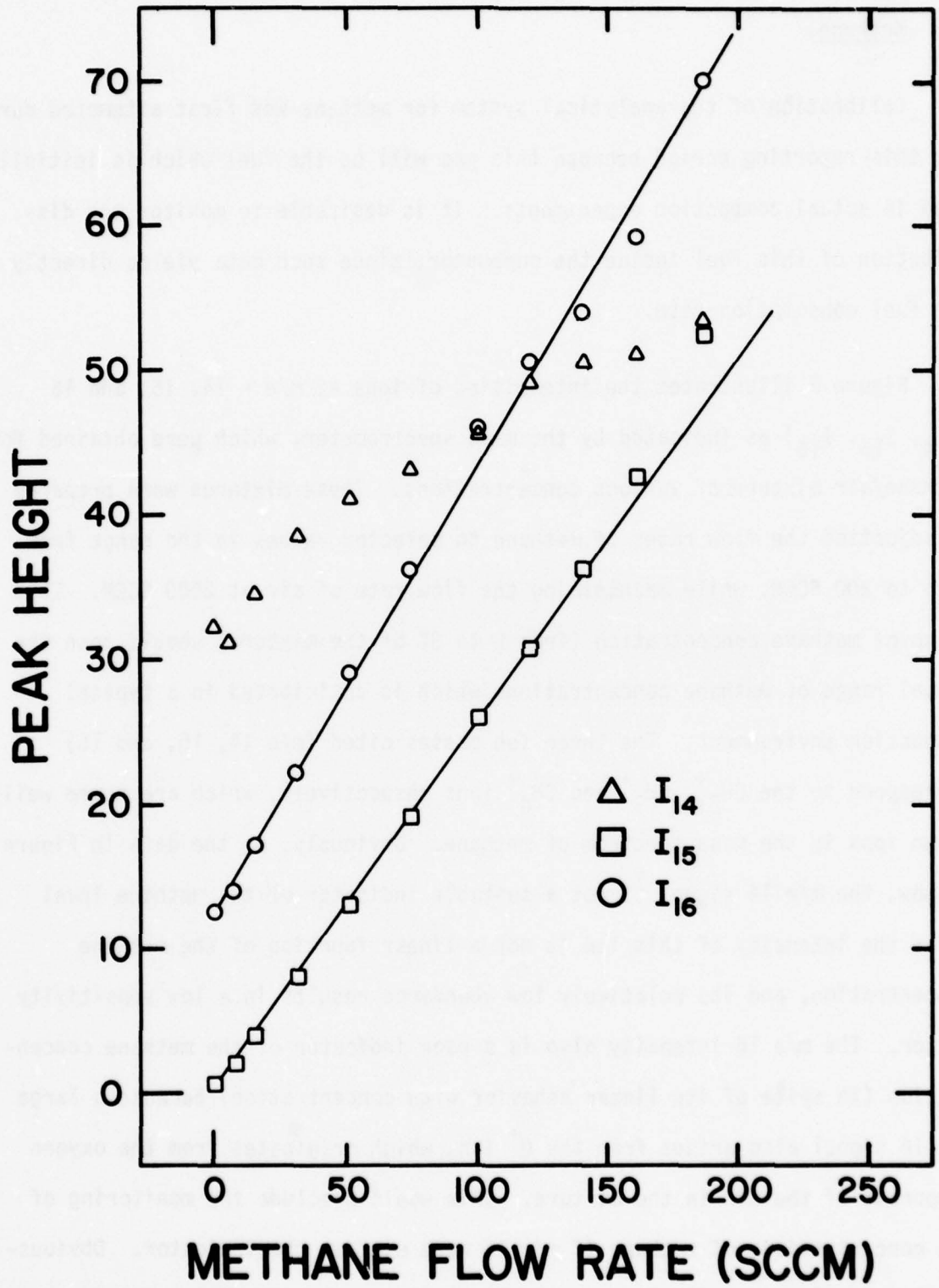

Figure 7. Intensities of Ions at m/e = 14,15, and 16 as a Function of Methane Flow Rate in a Methane/Air Mixture (Air Flow Rate 2000 SCCM)

minor contribution from the nitrogen ion, $^{15}N^+$, which arises from the nitrogen component in the air stream. Fortunately, the abundance of this ion in the mass spectrum is very small and its contribution to the m/e 15 can be ignored, provided that the methane constitutes more than 0.05% of the mixture. Also, since the $^{15}N^+$ contribution to m/e 15 is approximately constant when air is the major component of the mixture, the intensity of this ion signal can be subtracted from the total observed ion intensity at m/e = 15 to obtain the signal due only to CH_3^+.

Owing to the large fluctuations in temperature and total pressure which occur in a combustion environment (as well as occasional change of the mass spectrometric response) it is best to utilize the mass spectrometric detection system in a manner such that the ion intensity characteristic of any component to be measured can be monitored with reference to a component of the mixture which is essentially inert in the combustion process, such as nitrogen or argon. This requires that the mass spectrometer be operated in the multiple ion monitoring mode in which the indicator ion and the reference ion are measured simultaneously. The mole fraction of the component of interest is thus obtained with reference to an inert component to be selected. Relative mole fraction data, obtained in conjunction with temperature and pressure data measured at the sampling site, ultimately yield the absolute concentration of the component of interest.

For the present multiple ion monitoring experiments, the reference ion selected was Ar^+ (m/e = 40), which is present in natural air at a concentration of 0.934%. Thus, the I_{15} and I_{40} intensities were alternately monitored at the rate of one second per ion channel. A multichannel mass programmer was

used in these experiments, in a manner similar to that employed in the cold flow combustor gas sampling tests, which were described in the previous report.[1]

In the present calibration experiments, in which the flow rates of pure air $[(FR)_{air}]$ and methane $[(FR)_{methane}]$ were individually monitored, the mole fractions of methane $[(MF)_{methane}]$ and argon $[(MF)_{argon}]$ can be readily calculated, as follows:

$$(MF)_{methane} = \frac{[(FR)_{methane}]}{[(FR)_{air}] + [(FR)_{methane}]} \quad (1)$$

$$(MF)_{argon} = \frac{[(FR)_{air} \times 0.00934]}{[(FR)_{air}] + [(FR)_{methane}]} \quad (2)$$

Furthermore, the mass spectrometric signals, I_{15} and I_{40} are related to the flow rates in the following manner:

$$I_{15} - (I_{15})_o = k(CH_3^+)[(FR)_{methane}] + k(^{15}N^+)[(FR)_{air}](0.78) \quad (3)$$

$$I_{40} - (I_{40})_o = k(Ar^+)[(FR)_{air}](0.00934) \quad (4)$$

where $(I_{15})_o$ and $(I_{40})_o$ are the instrumental background signals at m/e 15 and m/e 40, (which can be obtained by setting the flows of both air and methane to zero) and $k(CH_3^+)$, $k(^{15}N^+)$ and $k(Ar^+)$ are the sensitivity factors per unit flow rate of methane, nitrogen and argon respectively.

Dividing equation (3) by equation (4) yields:

$$\frac{I_{15} - (I_{15})_o}{I_{40} - (I_{40})_o} = \frac{1}{0.00934} \frac{k(CH_3^+)}{k(Ar^+)} \frac{[(FR)_{methane}]}{[(FR)_{air}]}$$

$$+ \frac{0.78}{0.00934} \frac{k(^{15}N^+)}{k(Ar^+)} \qquad (5)$$

It is obvious from equations (1) and (2) that equation (5) can also be expressed in terms of the mole fractions of the gases. Making the appropriate substitution, one obtains,

$$\frac{I_{15} - (I_{15})_o}{I_{40} - (I_{40})_o} = \frac{k(CH_3^+)}{k(Ar^+)} \frac{[(MF)_{methane}]}{[(MF)_{argon}]} + \frac{0.78}{0.00934} \frac{k(^{15}N^+)}{k(Ar^+)} \qquad (6)$$

or,

$$\frac{(MF)_{methane}}{(MF)_{argon}} = \frac{k(Ar^+)}{k(CH_3^+)} \left[\frac{I_{15} - (I_{15})_o}{I_{40} - (I_{40})_o} - \frac{0.78}{0.00934} \frac{k(^{15}N^+)}{k(Ar^+)} \right] \qquad (7)$$

A plot of the measured values of $\left[\frac{I_{15} - (I_{15})_o}{I_{40} - I_{40})_o}\right]$ as a function of $\frac{(FR)_{methane}}{(FR)_{air}}$ used in the calibration experiment should yield a straight line having slope and intercept given by the relations,

$$\text{Slope} = \frac{1}{0.00934} \cdot \frac{k(CH_3^+)}{k(Ar^+)} \qquad (8)$$

$$\text{Intercept} = \frac{0.78}{0.00934} \cdot \frac{k(^{15}N^+)}{k(Ar^+)} \qquad (9)$$

Consequently, the mole fraction of methane relative to that of argon in the gas sampled from the combustion chamber can be readily obtained from the experimentally determined value of $\frac{I_{15} - (I_{15})_o}{I_{40} - (I_{40})_o}$, provided that calibration is

accomplished under experimental conditions identical to those of the combustor gas sampling.

Figures 8 to 10 show typical plots of ion intensity ratios (SRATIO) as functions of the flow rate ratios (FRATIO), obtained for various experimental conditions, as indicated in Table 2. Table 2 also lists the calibration coefficients, $\frac{k(CH_3^+)}{k(Ar^+)}$, and $\frac{k(^{15}N^+)}{k(Ar^+)}$, which were derived from these experiments. The data plotted in Figures 8 to 10 indicates that the ion intensity ratios do indeed vary linearly with the corresponding flow rate ratios, which is further supported by the calculated values of correlation coefficients. It is also seen from these results that the values of $\frac{k(CH_3^+)}{k(Ar^+)}$ derived are in reasonably good agreement over a wide range of air flow rate (from 1000 SCCM to 3000 SCCM). The agreement between the values of $\frac{k(^{15}N^+)}{k(Ar^+)}$ obtained in the experiments listed in Table 2 is rather poor, but comparison of these values is not really meaningful owing to the small magnitudes of the ratios.

2. Carbon Dioxide.

Carbon dioxide is one of the major products formed in most combustion processes. The monitoring of this product from the combustor is certainly of interest in the present project. Among the ions formed from carbon dioxide under electron impact, CO_2^+(m/e = 44) is the only reasonable choice for calibration purposes, since the other major ion in the mass spectrum, CO^+(m/e = 28), has the same nominal mass as the ion N_2^+ from nitrogen, which is also present in the combustor. These two ions cannot be distinguished by the quadrupole mass spectrometer which is presently employed since the mass resolution is not adequate.

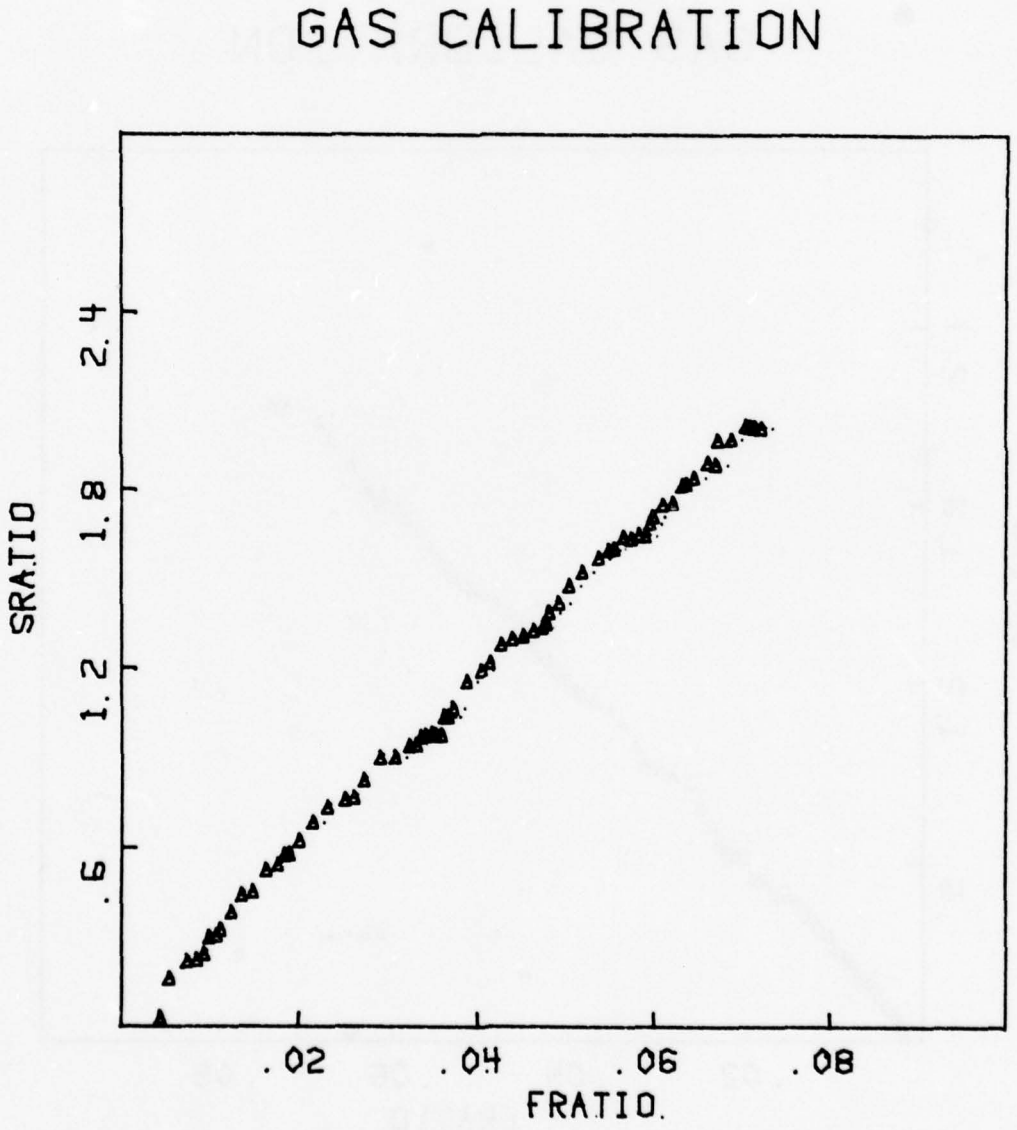

Figure 8. Plots of SRATIO As a Function of FRATIO for Air/ Methane Mixtures (See Table II for experimental conditions applicable to this figure)

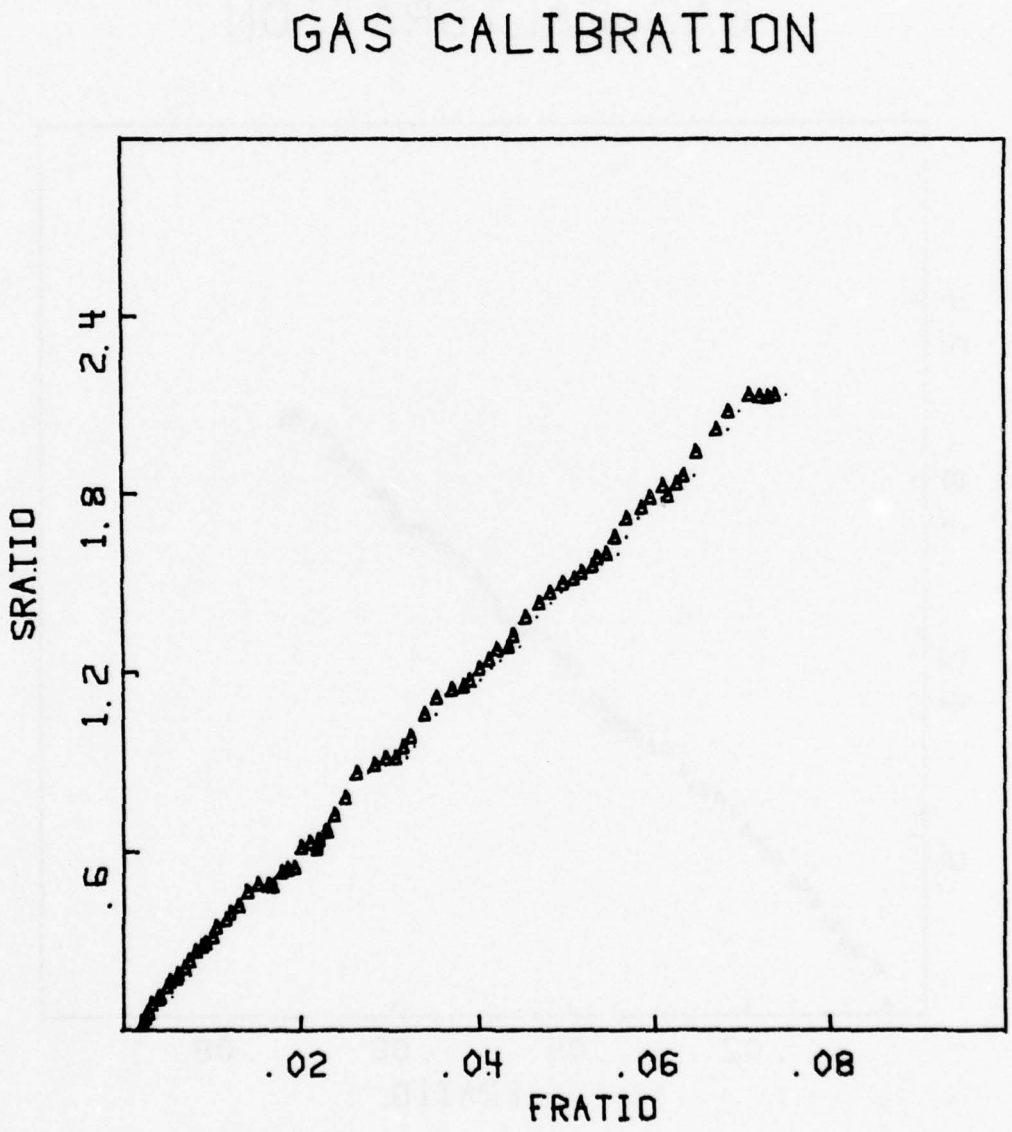

Figure 9. Plots of SRATIO As a Function of FRATIO for Air/Methane Mixtures (See Table II for experimental conditions applicable to this figure)

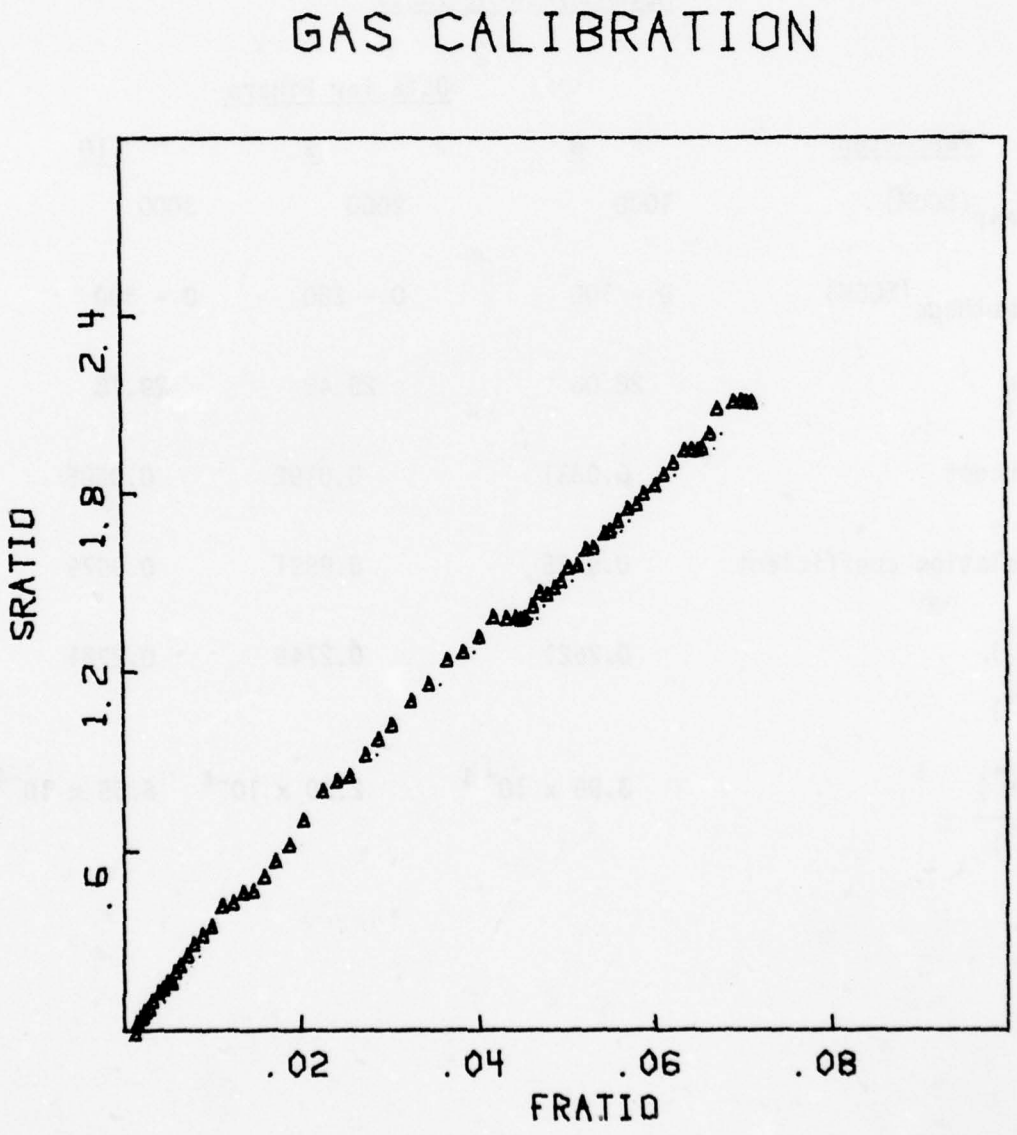

Figure 10. Plots of SRATIO As a Function of FRATIO for Air/Methane Mixtures (See Table II for experimental conditions applicable to this figure)

TABLE 2

EXPERIMENTAL PARAMETERS FOR GAS CALIBRATION EXPERIMENTS WITH METHANE/AIR MIXTURES

Parameter	Data for Figure 8	9	10
$(FR)_{air}$(SCCM)	1000	2000	3000
$(FR)_{methane}$(SCCM)	0 - 100	0 - 200	0 - 300
Slope	28.06	29.42	29.78
Intercept	0.0331	0.0192	0.0505
Correlation coefficient	0.9985	0.9991	0.9979
$\frac{k(CH_3^+)}{k(Ar^+)}$	0.2621	0.2748	0.2781
$\frac{k(^{15}N^+)}{k(Ar^+)}$	3.96×10^{-4}	2.30×10^{-4}	6.05×10^{-4}

The calibration procedure which was adopted for carbon dioxide is basically the same as that used for methane. That is, carbon dioxide/air mixtures, produced at various concentrations, by individually varying the flow rates of each component, are introduced into the mass spectrometer, and the ion intensities of I_{44} and I_{40} are alternately monitored using the multiple ion monitoring capability. The expressions relating the mole fractions of carbon dioxide and argon to the respective ion intensities are derived in the same manner as described earlier for methane. These are shown below:

$$(MF)_{CO_2} = \frac{[(FR)_{CO_2}] + [(FR)_{air}]\ (0.00033)}{[(FR)_{CO_2}] + [(FR)_{air}]} \tag{10}$$

$$(MF)_{Ar} = \frac{[(FR)_{air}]\ (0.00934)}{[(FR)_{CO_2}] + [(FR)_{air}]} \tag{11}$$

$$I_{44} - (I_{44})_o = k(CO_2^+)\left[[(FR)_{CO_2}] + [(FR)_{air}]\ \ (0.00033)\right] \tag{12}$$

$$I_{40} - (I_{40})_o = k(Ar^+)[(FR)_{air}]\ (0.00934) \tag{13}$$

Here, the constant, 0.00033 is the abundance of CO_2 present in natural air. Again, the above expressions yield,

$$\frac{I_{44} - (I_{44})_o}{I_{40} - (I_{40})_o} = \frac{1}{0.00934}\ \frac{k(CO_2^+)}{k(Ar^+)}\ \frac{[(FR)_{CO_2}]}{[(FR)_{air}]} + \frac{0.00033}{0.00934}\ \frac{k(CO_2^+)}{k(Ar^+)} \tag{14}$$

or

$$\frac{I_{44} - (I_{44})_o}{I_{40} - (I_{40})_o} = \frac{k(CO_2^+)}{k(Ar^+)}\ \frac{(MF)_{CO_2}}{(MF)_{Ar}} \tag{15}$$

Obviously, in this case also, a plot of the ratio, $\frac{I_{44} - (I_{44})_o}{I_{40} - (I_{40})_o}$, as a function

of the ratio $\frac{(FR)_{CO_2}}{(FR)_{air}}$, should yield a straight line, with the coefficient $\frac{k(CO_2^+)}{k(Ar^+)}$, being derivable from either the slope or the intercept of the line.

The results of the calibration experiments with CO_2 are presented in Figures 11 to 13, and the data are listed in Table 3. Again, the linearity of the plots are reasonable and the agreement in the values of $\frac{k(CO_2^+)}{k(Ar^+)}$ obtained from the slopes of these plots are acceptable. The rather poor agreement in the ratios obtained from the intercepts of these plots is partially due to the errors associated with the background subtraction process.

3. Oxygen

The monitoring of the oxygen (from air) concentration profile in a combustion chamber is just as important as monitoring of the fuel, since the former provides an indication of the combustion rate, irrespective of the final combustion products. The initial concentration of oxygen prior to combustion is readily obtainable, since the natural abundance of oxygen in air is 20%. Since the oxygen concentration during a combustion test is always lower than this initial value, a calibration procedure employing oxygen/air mixtures is not suitable. Therefore, nitrogen/air mixtures were used in the present calibration experiments.

The sample ion and reference ion for these experiments are O_2^+ (m/e + 32) and N_2^+ (m/e = 28) respectively. The expression relating the mole fractions and ion intensities for oxygen and nitrogen, analogous to those derived in the preceding sections are as follows.

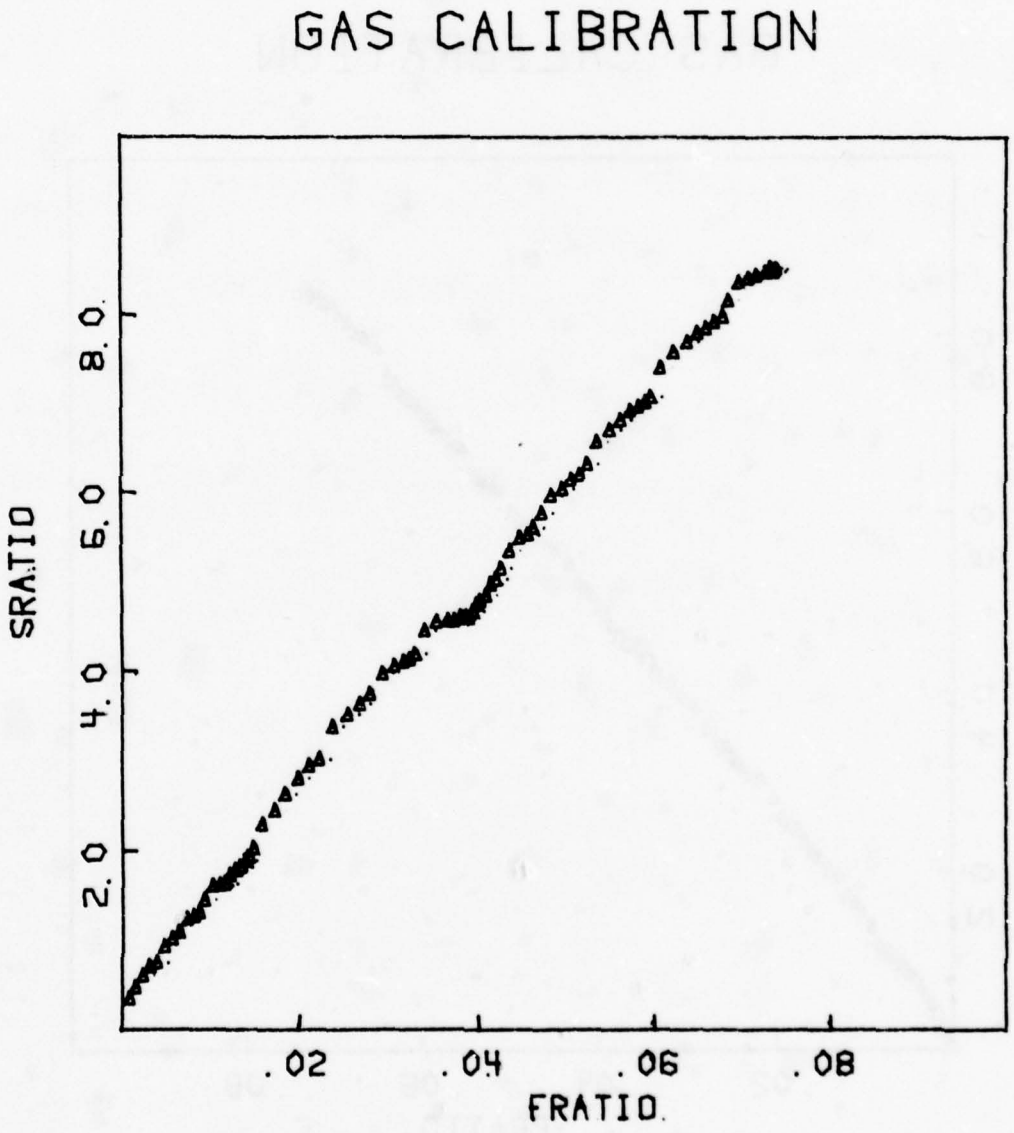

Figure 11. Plots of SRATIO As a Function of FRATIO for Carbon Dioxide/Air Mixtures (See Table III for experimental conditions applicable to this figure)

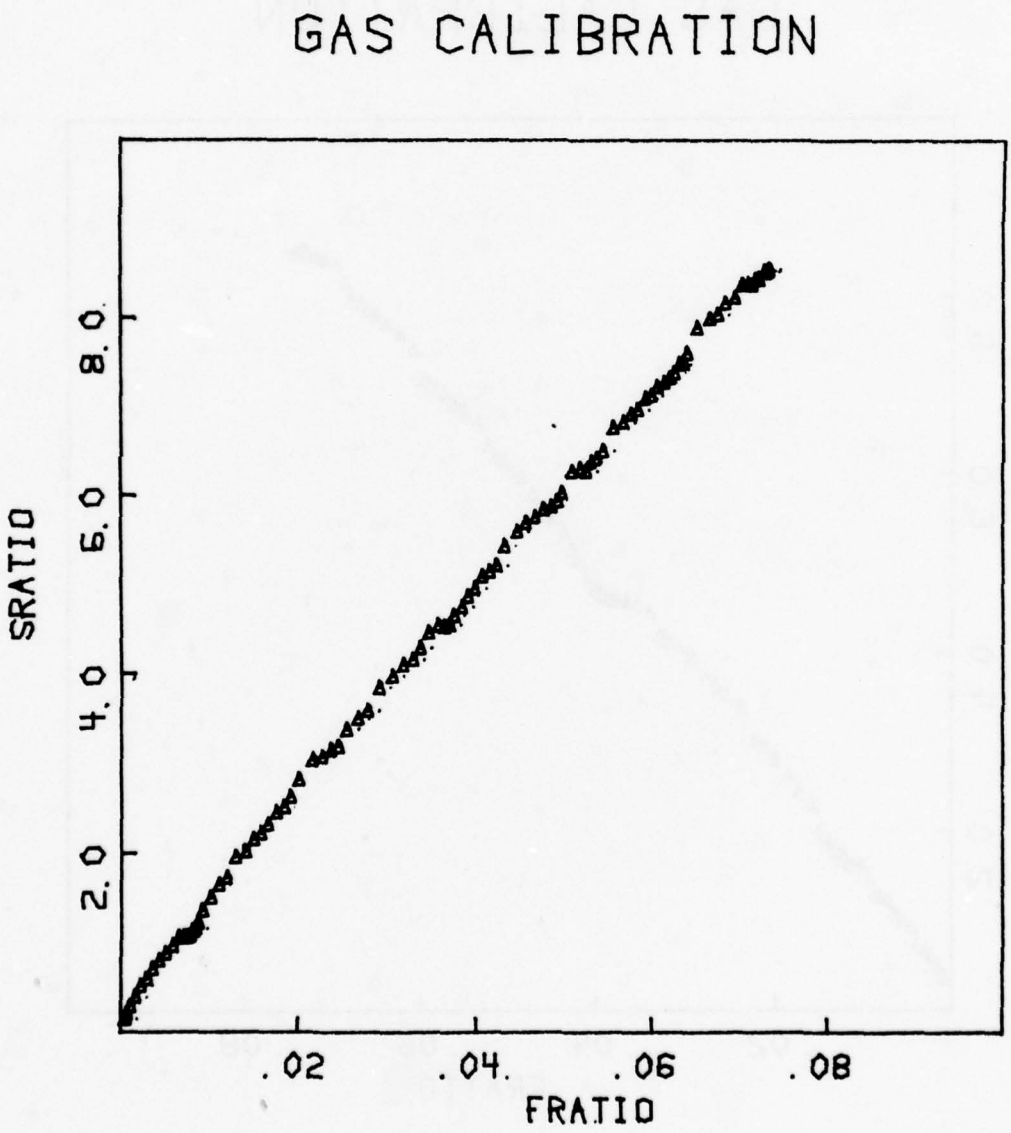

Figure 12. Plots of SRATIO As a Function of FRATIO for Carbon Dioxide/Air Mixtures (See Table III for experimental conditions applicable to this figure)

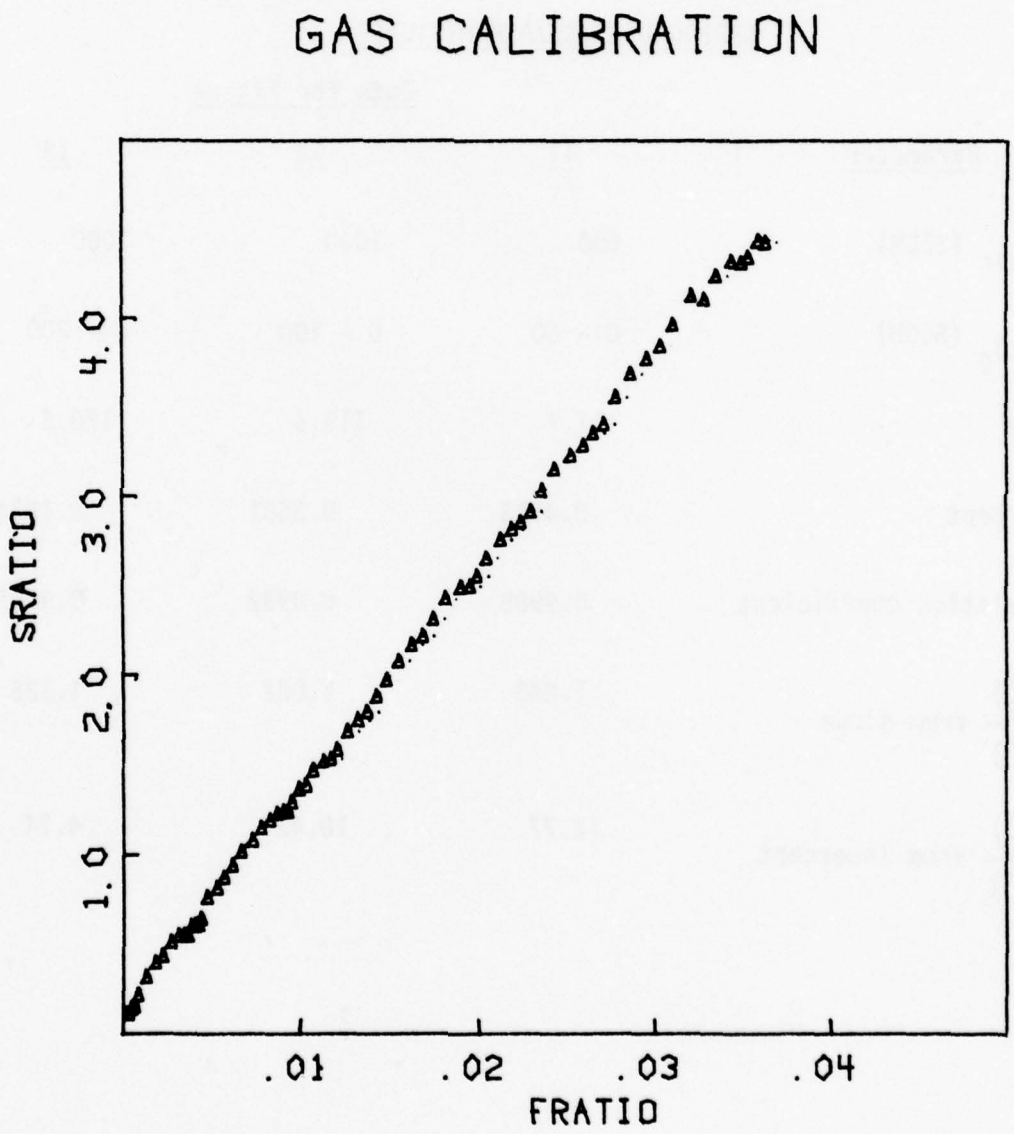

Figure 13. Plots of SRATIO As a Function of FRATIO For Carbon Dioxide/Air Mixtures (See Table III for experimental conditions applicable to this figure)

TABLE 3

EXPERIMENTAL PARAMETERS FOR GAS CALIBRATION EXPERIMENTS WITH CARBON DIOXIDE/AIR MIXTURES

Parameter	Data for Figure 11	12	13
$(FR)_{air}$ (SCCM)	500	1000	2000
$(FR)_{CO_2}$ (SCCM)	0 - 50	0 - 100	0 - 200
Slope	111.7	113.6	120.6
Intercept	0.4513	0.3681	0.1674
Correlation coefficient	0.9988	0.9992	0.9995
$\frac{k(CO_2^+)}{k(Ar^+)}$ from slope	1.043	1.061	1.126
$\frac{k(CO_2^+)}{k(Ar^+)}$ from intercept	12.77	10.42	4.74

$$(MF)_{O_2} = \frac{[(FR)_{air}] \quad (0.20)}{[(FR)_{air}] + [(FR)_{N_2}]} \tag{16}$$

$$(MF)_{N_2} = \frac{[(FR)_{N_2}] + [(FR)_{air}] \ (0.79)}{[(FR)_{air}] + [(FR)_{N_2}]} \tag{17}$$

$$I_{32} - (I_{32})_o = k(O_2^+) \ [(FR)_{air}] \ (0.20) \tag{18}$$

$$I_{28} - (I_{28})_o = k(N_2^+) \ [(FR)_{N_2}] + [(FR)_{air}](0.79) \tag{19}$$

$$\frac{I_{28} - (I_{28})_o}{I_{32} - (I_{32})_o} = 5\frac{k(N_2^+)}{k(O_2^+)} \frac{[(FR)_{N_2}]}{[(FR)_{air}]} + \frac{0.79}{0.20} \frac{k(N_2^+)}{k(O_2^+)}$$

$$= \frac{k(N_2^+)}{k(O_2^+)} \quad \frac{(MF)_{N_2}}{k(MF)_{O_2}} \tag{20}$$

As seen previously, a plot of the ion intensity ratio (SRATIO) indicated in Equation (20) as a function of the corresponding flow rate ratio (FRATIO), will yield a straight line. Both the slope and intercept of this line will yield the sensitivity coefficient ratio, $k(O_2^+)/k(N_2^+)$. The results of these calibration experiments are presented in Figures 14 through 18, and the relevant experimental parameters are listed in Table 4. As can be seen, the coefficient ratios derived from both the slopes and intercepts of the plots shown in Figures 14 - 18 are in good agreement.

4. Carbon Monoxide

Carbon monoxide is also a major product commonly formed in many combustion processes. The most abundant ion in the mass spectrum of this compound is CO^+ (m/e = 28), which, unfortunately, has the same nominal mass as the N_2^+ ion. The intensity of the latter is, of course, orders of magnitude larger than that of the CO^+ ion, and in addition, these two ions cannot be distinguished by the mass spectrometer presently employed. In one preliminary attempt at calibration for CO, a standard mixture containing 10% CO and 90% Ar was mixed with

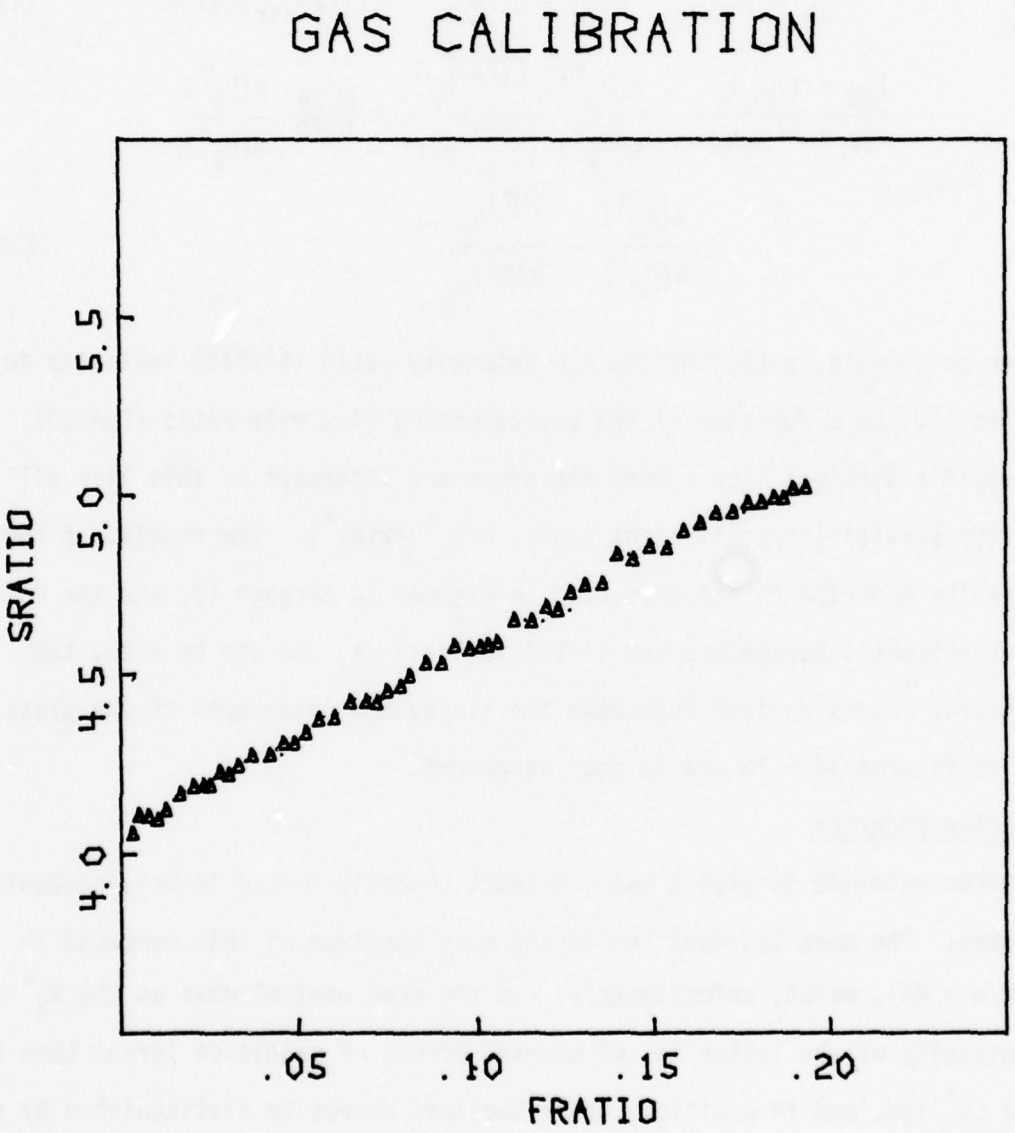

Figure 14. Plots of SRATIO As a Function of FRATIO for Nitrogen/Air Mixtures (See Table IV for experimental conditions applicable to this figure)

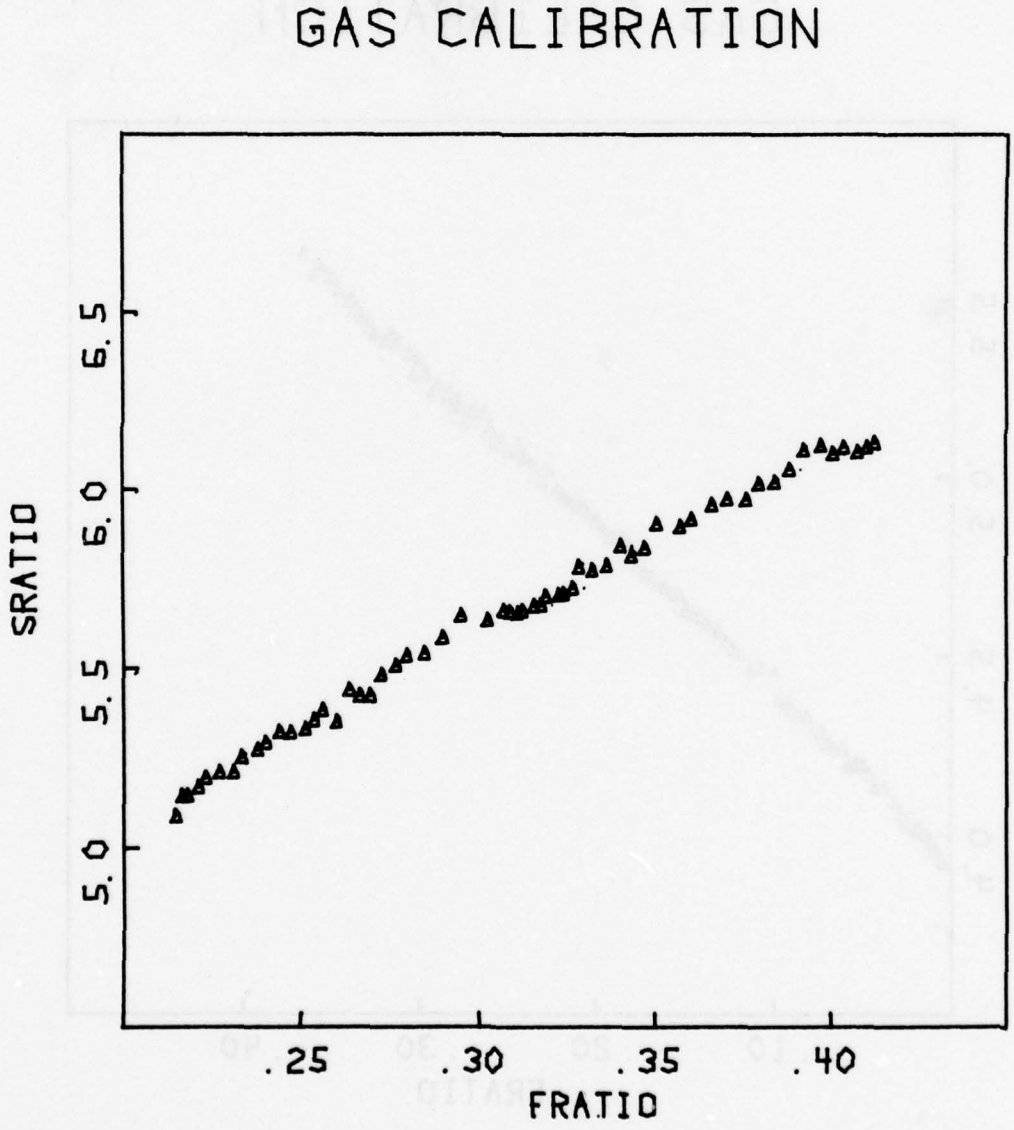

Figure 15. Plots of SRATIO As a Function of FRATIO for Nitrogen/Air Mixtures (See Table IV for experimental conditions applicable to this figure)

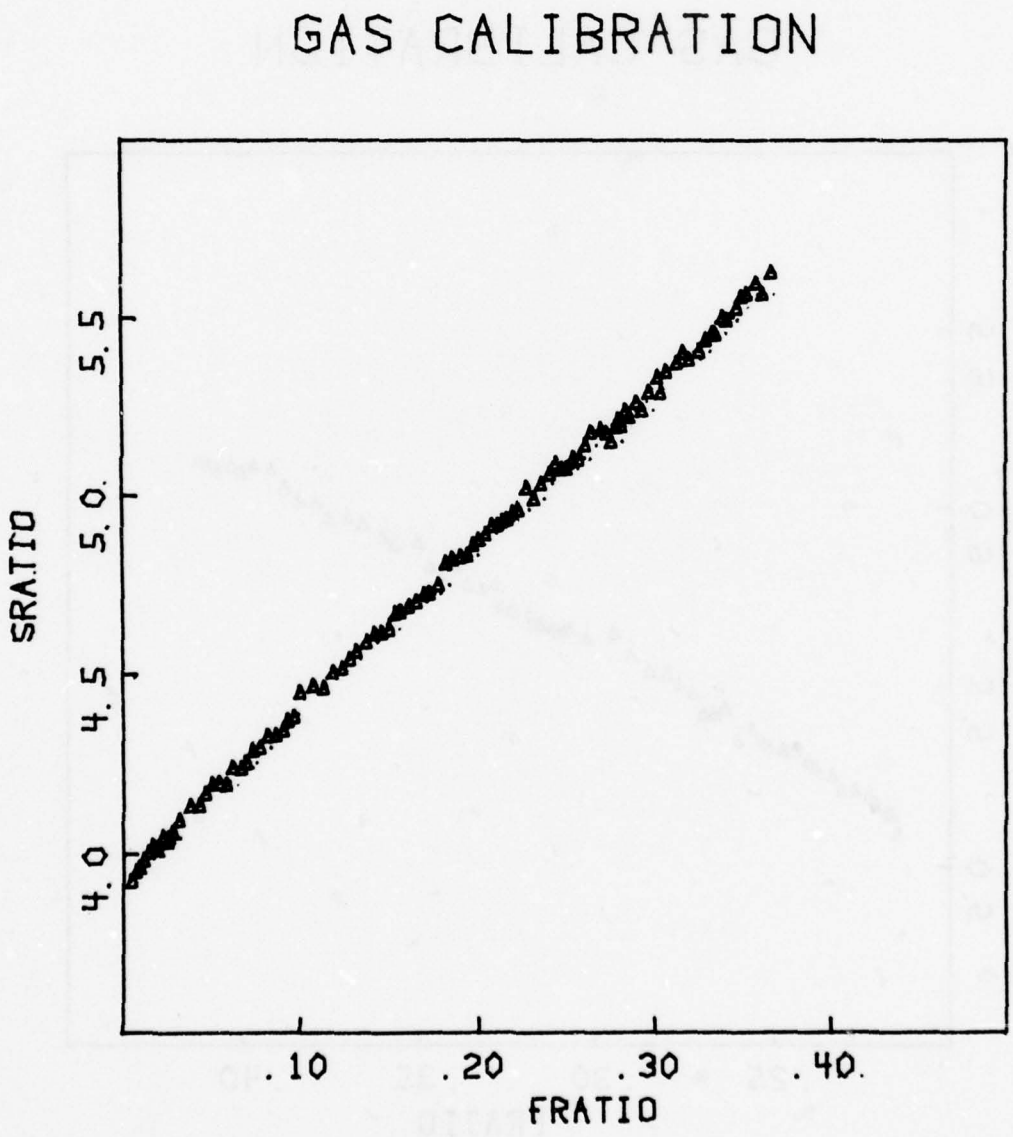

Figure 16. Plots of SRATIO As a Function of FRATIO for Nitrogen/Air Mixtures (See Table IV for experimental conditions applicable to this figure)

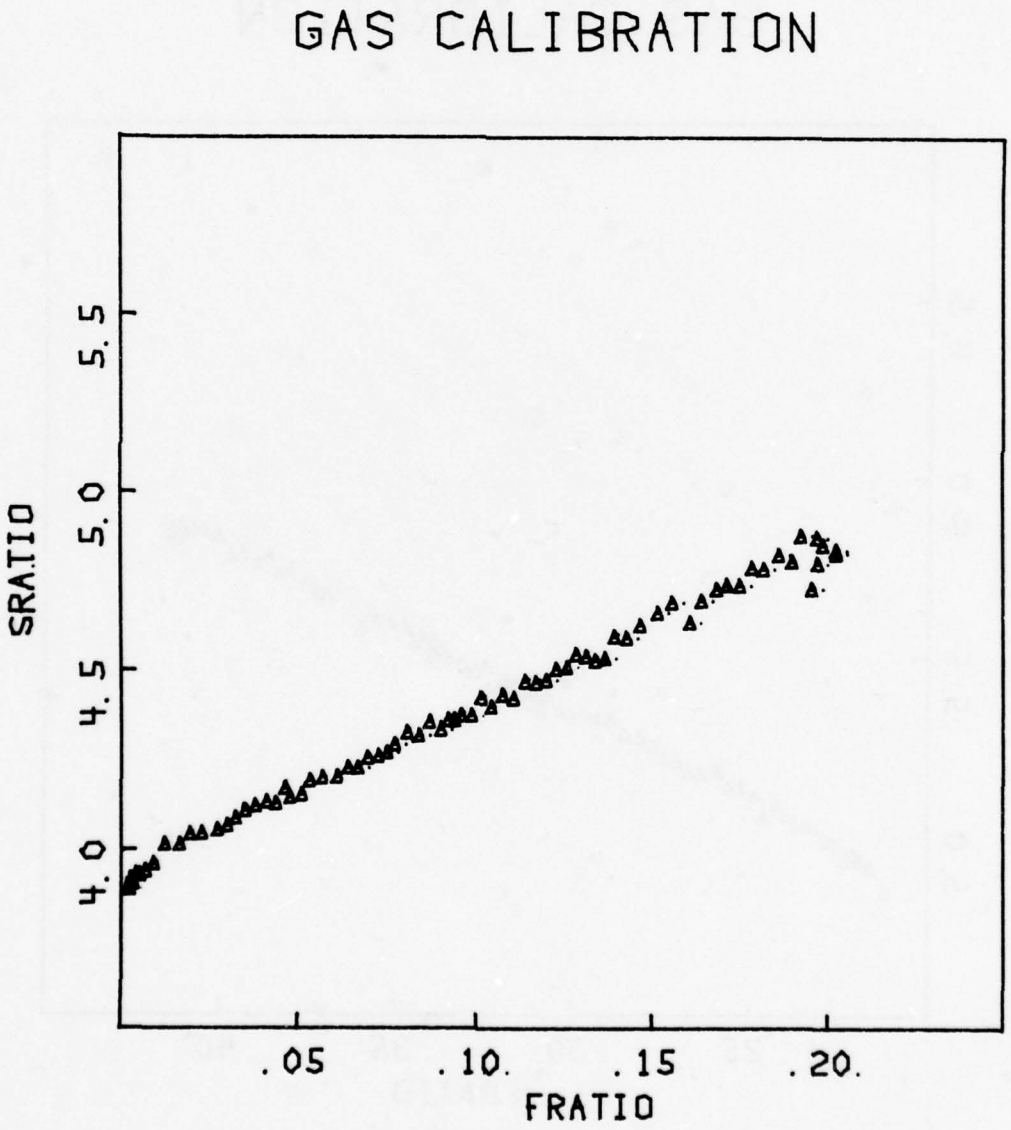

Figure 17. Plots of SRATIO As A Function of FRATIO for Nitrogen/Air Mixtures (See Table IV for experimental conditions applicable to this figure)

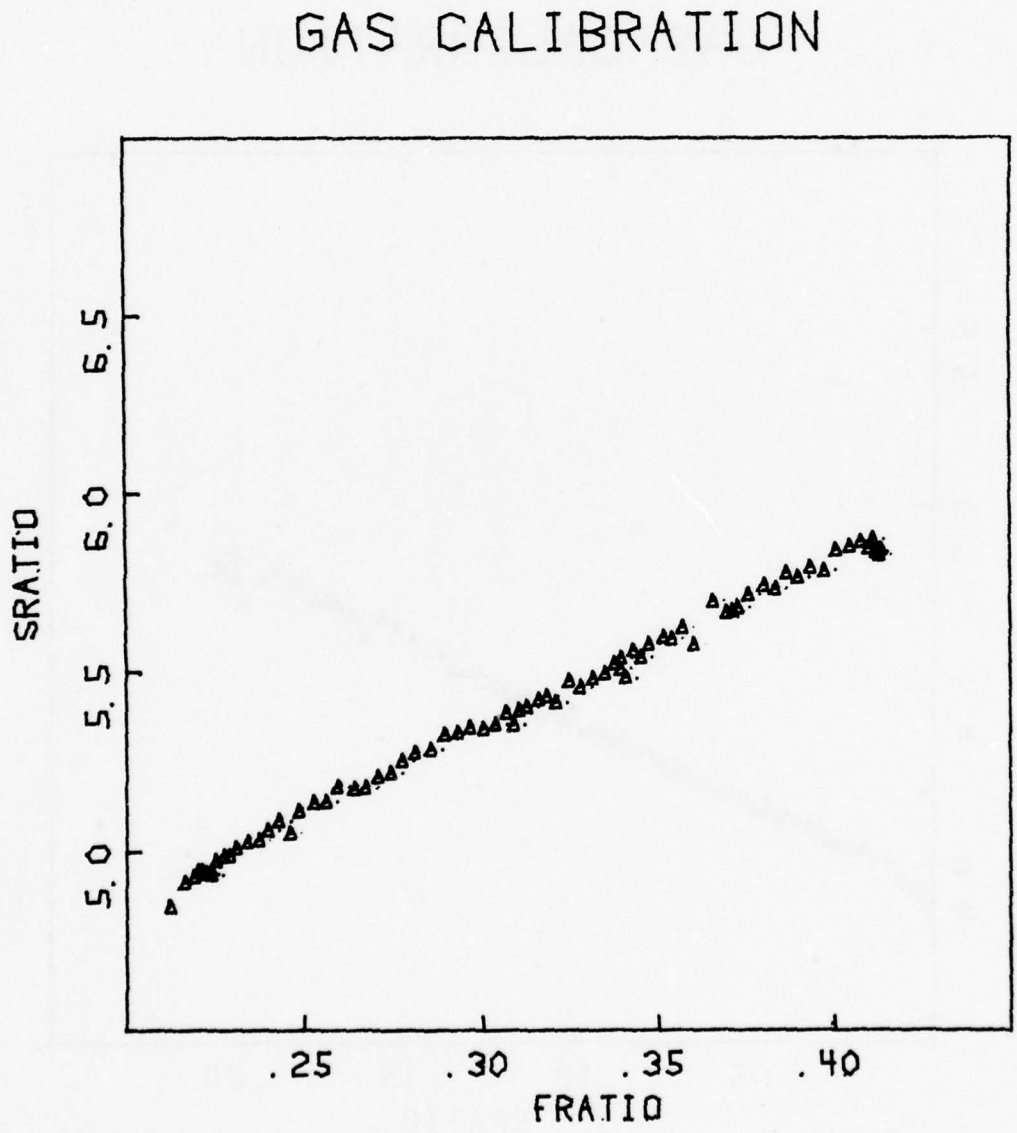

Figure 18. Plots of SRATIO As a Function of FRATIO for Nitrogen/Air Mixtures (See Table IV for experimental conditions applicable to this figure)

TABLE 4

EXPERIMENTAL PARAMETERS FOR GAS CALIBRATION EXPERIMENTS WITH NITROGEN/AIR MIXTURES

	Data for Figure				
Parameter	14	15	16	17	18
Air Flow Rate (SCCM)	1000	1000	1000	2000	2000
N_2 Flow Rate (SCCM)	0 - 200	200 - 400	0 - 400	0 - 400	400 - 800
Slope	5.06	5.16	4.52	4.65	4.77
Intercept	4.08	4.05	3.95	3.93	3.91
Correlation coefficient	0.9983	0.9963	0.9992	0.9963	0.9972
$\frac{k(O_2^+)}{k(N_2^+)}$ from slope	0.988	0.969	1.106	1.075	1.048
$\frac{k(O_2)}{k(N_2^+)}$ from intercept	0.968	0.975	1.000	1.005	1.010

air, and the m/e 28 ion was monitored by the mass spectrometer. The observed ion intensities, I_{28}, and I_{32}, can be expressed as follows:

$$I_{28} - (I_{28})_o = k(N_2^+)\,[(FR)_{air}]\,(0.79) + k(CO^+)\,[(FR)_{CO/Ar}]\,(0.1) \quad (21)$$

$$I_{32} - (I_{32})_o = k(O_2^+)\,[(FR)_{air}]\,(0.20) \quad (22)$$

Or, alternatively,

$$\frac{I_{28} - (I_{28})_o}{I_{32} - (I_{32})_o} = \frac{0.79}{0.20}\,\frac{k(N_2^+)}{k(O_2^+)} + \frac{0.1}{0.2}\,\frac{k(CO^+)}{k(O_2^+)}\,\frac{[(FR)_{CO/Ar}]}{[(FR)_{air}]} \quad (23)$$

The slope of the plot of the ion intensity ratio as a function of the gas flow rate ratio should yield the ratio of the sensitivity factors, $k(CO^+)/k(O^+)$, while the intercept will yield the ratio, $k(N_2^+)/k(O_2^+)$, which can also be obtained independently from the previous calibration. The relationship between the ion intensity ratio thus obtained and the relative mole fraction of CO in a combustor gas sample can be expressed then as,

$$\frac{I_{28} - (I_{28})_o}{I_{32} - (I_{32})_o} = \frac{(0.79)}{(0.20)}\,\frac{k(N_2^+)}{k(O_2^+)} + \frac{k(CO^+)}{k(O_2^+)}\,\frac{(MF)_{CO}}{(MF)_{O_2}}$$

$$= \frac{(0.79)}{(0.20)}\,\frac{k(N_2^+)}{k(O_2^+)} + \frac{k(CO^+)}{k(O_2^+)}\,\frac{(MF)_{N_2}}{(MF)_{O_2}}\,\frac{(MF)_{CO}}{(MF)_{N_2}} \quad (24)$$

This expression should, in principle, yield the mole fraction of CO relative to that of the inert gas, N_2, provided that the calibration is successfully accomplished and that the $(MF)_{O_2}/(MF)_{N_2}$ term is also obtained independently for the same sampling experiment. Unfortunately, the experimental errors involved in the calibration process proved to be too large to be acceptable for mixtures containing less than 1-2% of CO. Concentrations on this order are expected for typical combustion experiments to be studied in future experiments In view of these limitations, further calibration experiments were not conducted during the present reporting period. It should be noted, however, that

a novel technique involving the application of chemical ionization mass spectrometry for the monitoring of carbon monoxide is also actively being investigated in separate experiments being conducted at Wright State University. These studies will be described elsewhere.

5. Water

Although water is also among the major products in a combustion process, the procedures for successful monitoring of this product have not been established at this stage. The possibility of condensation, as well as surface adsorption of the sampled water vapor on the walls of the sampling probe and the transfer line connecting the probe to the mass spectrometer source are formidable problems which must be resolved. A good sampling probe must be designed so that substantial cooling occurs at the probe tip, in order to prevent any further chemical reactions from occurring after the sampled species are removed from the sampling point. However, excessive cooling at the tip of the probe may also cause condensation of compounds such as water vapor, and this would obviously yield erroneous concentration data. In order to minimize condensation and sorption of water vapor in the transfer line, this line must be heated to a sufficient temperature to maintain the water in the vapor phase.

Significant problems were also encountered in attempting to calibrate the mass spectrometer signal response for mixtures containing known quantities of water. Preparation of such mixtures is in itself a major task. With the present experimental arrangement, (see Figure 3) water must be introduced into a reservoir in liquid form, and then injected into the air stream in the manifold (n), which is heated to 230^{o}C. The first difficulty encountered during early stages of testing was in obtaining a steady flow of water,

as indicated by the rotometer, (l) which is designed to measure the flow rate of water in the liquid phase, over the range from 0 to 1.4 cc/min. Water vapor bubbles were repeatedly observed in the rotometer column, which caused large fluctuations in the meter reading. This problem was finally solved by pressurizing the water reservoir (m) to 30 psig and installing a metering valve downstream of the rotometer, while leaving the valve (f) fully open.

The ion which is monitored as an indicator of water is H_2O^+ (m/e = 18), which is not expected to be populated by any other significant compound present in the combustion gas environment. Unfortunately, the intensity of this ion was found to fluctuate excessively for any water flow rates employed in these experiments. These fluctuations were also accompanied by frequent sudden increases in the mass spectrometer ion source pressure. This clearly indicates that the water introduced did not vaporize in a continuous manner, in spite of the relatively high temperatures at which the walls of the tubing were maintained. These pressure fluctuations, are probably attributable to insufficient heating of the manifold in the area where liquid water is injected. It is possible that a water droplet is formed at the tip of the injection port and slowly grows in size until it is blown off by the incoming heated air stream, which then causes a sudden increase in the water concentration, and in turn in the m/e 18 ion intensity. In later experiments, a stainless steel wire coil filled with glass wool was inserted along the entire length of the manifold. This modification resulted in largely eliminating the pressure fluctuations and the m/e 18 signal was then found to be stable within 20%, for a period of about 5 minutes. Other improvements in

calibration system will probably be necessary in order to achieve greater stability for calibration of the mass spectrometer for the water signal response. With the present arrangement, only the lines carrying water between the injection port and the prechamber are heated to 230°C. It may be desirable that the prechamber itself, as well as the tubing within the chamber, also be heated.

Recently,a new approach to the water calibration problem was tested. With this method calibration was accomplished by simply monitoring the water ion signal (m/e = 18) as a function of the source pressure. It was determined that, in spite of fluctuations in both the water flow rate and in the water pressure in the ion source, the observed m/e = 18 (H_2O^+) ion intensity always correlated linearly with the actual water pressure in the ion source. By comparing the observed H_2O^+ ion signal with the response for some reference ion such as N_2^+ from air, one can thus derive the relative sensitivity factor for water, that is, $I_{18}/P_{H_2O}/I_{28}/P_{air}$. A value of 0.99 was determined for this factor for one particular set of mass spectrometer conditions, and for a range of source pressures which correspond to those expected for experiments in which combustor gas is sampled. This type of calibration, as a substitute of the more rigorous calibration procedure based on actual water flow rate, is acceptable only if the discrimination factor for the sampling of water from the combustor can be separately assessed. Unfortunately, it is unlikely that this discrimination factor can be obtained with a high degree of accuracy.

6. Oxides of Nitrogen

Two oxides of nitrogen believed to be formed during the combustion process of interest for this project are nitric oxide and nitrogen dioxide. The monitoring of these gases is of importance mainly from the standpoint of assessing environmental pollution effects arising from operation of the combustor. The analyses of these gases are difficult, especially for nitric oxide, because of its low concentration (parts per million) in the combustion exhaust. No calibration work for these gases has yet been conducted using the newly constructed gas calibration system. However, some preliminary work was accomplished in monitoring nitric oxide at the parts-per-million level in an earlier stage, utilizing the available facility. A brief report describing the results of this work is attached in the Appendix of this report.

SECTION V

SAMPLING OF GASEOUS SPECIES FROM A BURNER FLAME

Prior to conducting actual monitoring of gaseous species in a reactive combustor system, it is desirable to test the existing gas monitoring apparatus with a smaller-scale reactive combustion environment. A flat flame burner, for which the flame characteristics and the combustion product distributions have already been well established in several instances, is ideally suited for this purpose. This will also permit an assessment of various probe designs, and yield an indication of the overall capabilities of the analytical system, in its present design, for monitoring reactive environments.

While awaiting the acquisition of a flat flame burner to be used for future tests, a regular Bunsen burner was acquired and set up for preliminary flame sampling tests. This burner was connected to a methane cylinder via a metering valve and a linear mass flow meter, which are parts of the existing gas calibration system. Combustion tests were conducted in the ambient atmosphere with various methanol flow rates, ranging from 1000 SCCM to 2000 SCCM. The exhaust of the flame was readily vented through the existing building venting system.

For the purpose of flame sampling, a quartz microprobe was fabricated and connected to the mass spectrometer inlet via flexible tubing. For comparison, some sampling tests were also conducted with a stainless steel probe. However, owing to the fact that this probe was not equipped with a water cooling system, each experiment had to be limited to a few minutes of sampling time. In these preliminary tests, the teflon tubing served as the connecting line.

The lack of a flame stabilization system in these initial tests resulted in excessive fluctuations in the flame zone and it was not possible to obtain any meaningful concentration profiles for the flame species. Therefore, these initial sampling experiments were only conducted with the probe tip located at three different positions, generally along the centerline of the burner flame. The first probe position was at the level immediately above the burner outlet, which should give data indicative of the initial fuel concentration prior to combustion. The second and third probe positions were located at 3 and 4 cm respectively, above the burner outlet. These two positions generally correspond to the inner and outer regions, respectively, of the flame zone.

During sampling, the mass spectrometer was interfaced with the computer system

which was operated in the high speed integration mode. The six available channels of the mass programmer were tuned to m/e = 14, 15, 18, 32, 40 and 44. Ion masses 14 and 40 correspond to the N^+ and Ar^+ ions, which represent the concentrations of two gases (N_2 and Ar) which are unreactive in the combustion environment. Consumption of the fuel (CH_4) and oxygen are monitored by the measurements of the CH_3^+ (m/e 15) and O_2^+ (m/e = 32) ions, respectively, while the flame products, CO_2 and water, are detected by monitoring the CO_2^+ (m/e = 44) and H_2O^+(m/e = 18) ions, respectively. All six channels were monitored sequentially in rapid succession in these tests, with the dwell time for each channel adjusted to approximately 0.1 sec. A plot of all six ion intensities as a function of time reveals that during flame fluctuations, the ion current signals are severaly distorted from their normal values, and the data obtained during such fluctuations must obviously be discarded. However, it was found that during a typical flame sampling period, lasting for about 60 seconds, data obtained during approximately half of the total sampling period were reasonably steady and were acceptable for use in quantitative analysis.

Figure 19 shows three mass spectra of the gaseous species sampled from the flame by the quartz microprobe. The three spectra correspond to three separate sampling experiments in which the probe tip was located below (zone 1), within (zone 2), and above (zone 3) the flame, respectively. The mass spectrum of species sampled from zone 1 represents that of the mixture of air and methane fuel prior to combustion. This spectrum includes ions characteristic of air, N_2^+, O_2^+, and Ar^+, and ions produced from methane such as CH_3^+ and CH_4^+. The mass spectrum of the species from zone 2 is also seen to include the methane ions (CH_3^+ and CH_4^+) but the O_2^+ ion is completely absent, indicating a depletion of oxygen as a result

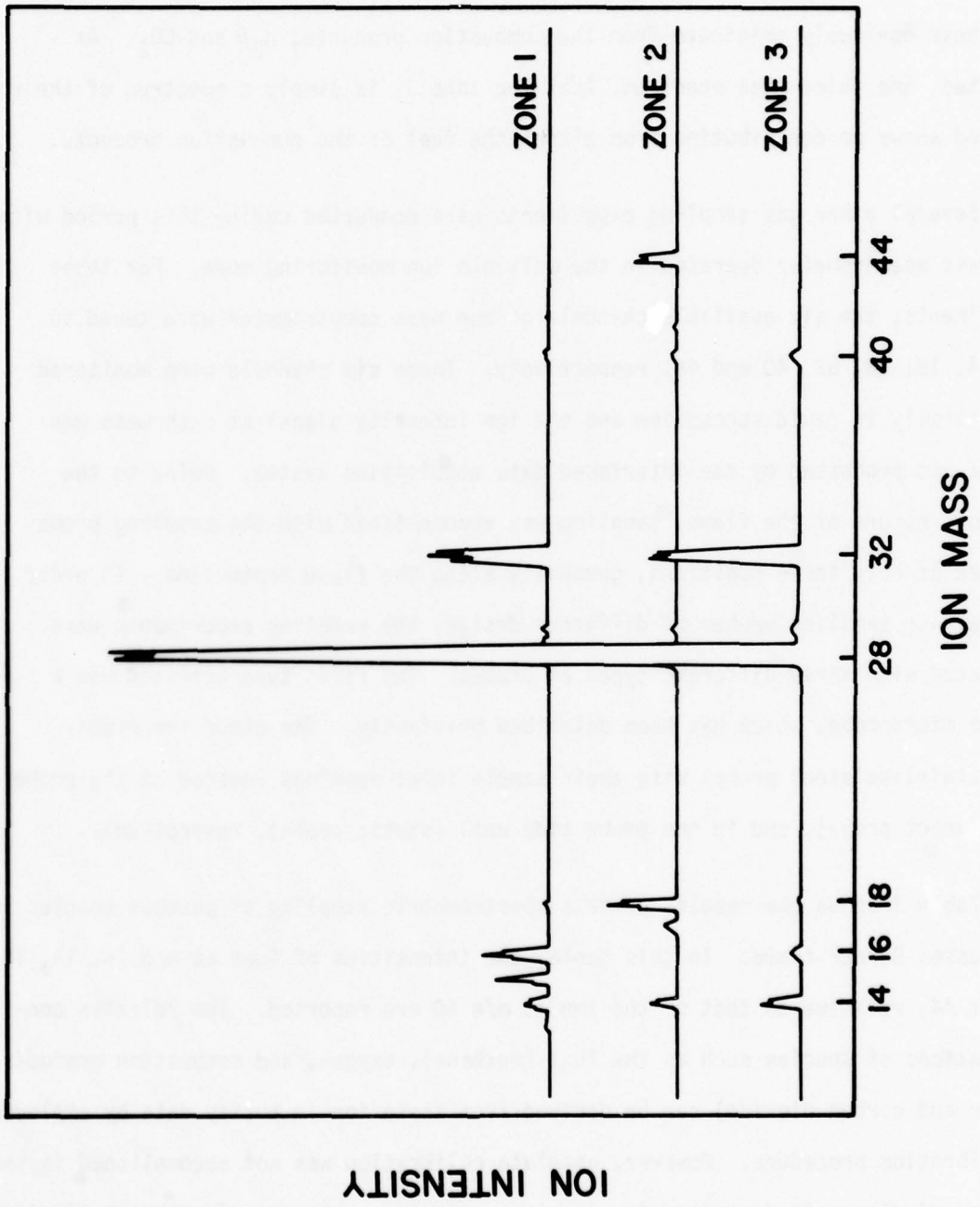

Figure 19. Mass Spectra of the Gaseous Species Sampled from the Bunsen Burner Flame by the Quartz Microprobe

of combustion. Concurrently, the ions OH^+, H_2^+, and CO_2^+ appear on the mass spectrum, and these obviously originate from the combustion products, H_2O and CO_2. As expected, the third mass spectrum, that for zone 3, is simply a spectrum of the room air and shows no contribution from either the fuel or the combustion products.

Several other gas sampling experiments were conducted during this period with the mass spectrometer operated in the multiple ion monitoring mode. For these experiments, the six available channels of the mass spectrometer were tuned to m/e 14, 15, 18, 32, 40 and 44, respectively. These six channels were monitored sequentially in rapid succession and the ion intensity signal at each mass was stored and processed by the interfaced data acquisition system. Owing to the unstable nature of the flame, sampling was accomplished with the sampling probe located at only three positions, generally along the flame centerline. In order to evaluate sampling probes of different design, the sampling experiments were conducted with three different types of probes. The first type utilized was a quartz microprobe, which has been described previously. The other two probes were stainless steel probes with their sample inlet openings located at the probe tip (impact probe), and in the probe side wall (static probe), respectively.

Table 5 shows the results of mass spectrometric sampling of gaseous species in the Bunsen Burner flame. In this table, the intensities of ions at m/e 14, 15, 18, 32 and 44, relative to that of the ion at m/e 40 are reported. The relative concentrations of species such as the fuel (methane), oxygen, and combustion products (water and carbon dioxide) can be derived from these ion intensity data by employing a calibration procedure. However, absolute calibration was not accomplished in the present studies. As described in previous reports, because of enormous fluctuations in the primitive burner flame used for the preliminary sampling experiments, the data obtained are not sufficiently accurate to warrant further detailed quantita-

Table 5

RESULTS OF MASS SPECTROMETRIC SAMPLING OF GASEOUS SPECIES IN A BUNSEN BURNER FLAME

Probe Type	Probe Location[a] (cm)	Relative Ion Intensities[b] at m/e				
		14	15	18	32	44
Quartz microprobe	0	4.57	7.05	0.40	14.37	0.06
	3	3.94	0	10.75	0.94	7.00
	4	4.18	0	10.51	0.99	8.00
Stainless-Steel impact probe	0	4.23	5.00	2.80	11.73	0.82
	3	3.47	0.04	7.12	0	6.91
	4	3.25	0.05	7.82	0.05	8.27
Stainless-Steel static probe	0	3.35	5.15	1.95	8.68	0.43
	3	2.13	0.32	7.60	0.03	4.11
	4	1.95	0.36	6.95	0.04	7.20

a. Values indicate the vertical distance between the probe inlet opening and the burner baseline.

b. Values indicate the intensity of the ion at given m/e, relative to that of ion at m/e 40. Each value is the average of two independent runs.

tive analysis.

Toward the end of this contracting period, a flat flame burner was acquired on tempo.ary loan from another division of the AFAPL. This burner has an inner and outer flame region with the flows of the fuel and air for these two regions independently controlled and premixed prior to burning. The burner head is water-cooled and shielded with an outer argon layer to further enhance the stability of the flame. This burner is presently installed at the site of the mass spectrometric monitoring system with all the gas flow lines properly connected. However, further work is still required in order to accomplish the proposed gas sampling experiments. The major task remaining involves the fabrication of a burner housing system which will facilitate 1) pumping of the flame zone; 2) precise control of the pressure of the burner housing; 3) control and measurement of the position of the sampling probe which is to traverse along a direction either parallel to, or perpendicular to the flame front; and 4) interfacing the sampling probe with the mass spectrometric monitoring system.

APPENDIX

IN-SITU MEASUREMENTS OF NITRIC OXIDE (NO) CONCENTRATIONS AT PARTS-PER-MILLION LEVELS

Cherng Chang, Gary D. Sides, and Thomas O. Tiernan

Department of Chemistry
Wright State University
Dayton, Ohio 45431

TABLE OF CONTENTS

INTRODUCTION

Rapid advances in the state-of-the-art of mass spectrometry in recent years have resulted in widespread applications of this analytical tool for on-line monitoring and diagnostics. One example of such analytical applications is typified by research currently in progress under the sponsorship of the Air Force Aero Propulsion Laboratory at Wright-Patterson Air Force Base. In this research, a quadrupole mass spectrometer has been successfully employed as a diagnostic tool, for in-situ measurements of gas species concentrations in a simulated combustor device. In this combustor, compressed air is mixed with trace quantities of simulated fuel (argon) at a total pressure of several atmospheres, and a flow speed approaching that of sound. Argon/air mixing profiles within the combustor chamber under various experimental conditions can be obtained using this in-situ gas analysis system.

The work described in this report represents the results of preliminary experiments conducted with the same instrumentation, in an effort to determine the feasibility of monitoring nitric oxide. These results clearly demonstrate the applicability of these techniques for the measurement of nitric oxide (NO) concentration in a flow field at parts-per-million levels.

EXPERIMENTAL

Figure A-1 shows schematically the gas sample preparation manifold and the mass spectrometric gas inlet system employed in the present work. With the exception of minor changes in the sample preparation system, the apparatus is essentially the same as described earlier and utilized previously in the APL program. Using this system, a mixture of NO-in-air or NO-in-argon at various concentration levels can be readily prepared. As shown in the figure, the mixture is prepared by mixing the buffer gas (argon or compressed air) with a standard NO/N_2 mixture containing 2000 ppm of NO. The flow rate of each gas is closely controlled by the opening of the variable leak valve, and is monitored by the linear flow meter shown in the figure. The final mixture of known concentration is then introduced into the mass spectrometer gas inlet system.

The gas inlet system illustrated in Figure A-1 is merely a differential pumping system which limits the amount of gas sample admitted to the mass spectrometer ion source. The degree of differential pumping can be controlled to provide a suitable ion source pressure, simulating the actual condition for sampling of gas from a flow field.

The gas analysis system is a standard Extranuclear quadrupole mass spectrometer which is equipped with a mass programmer,

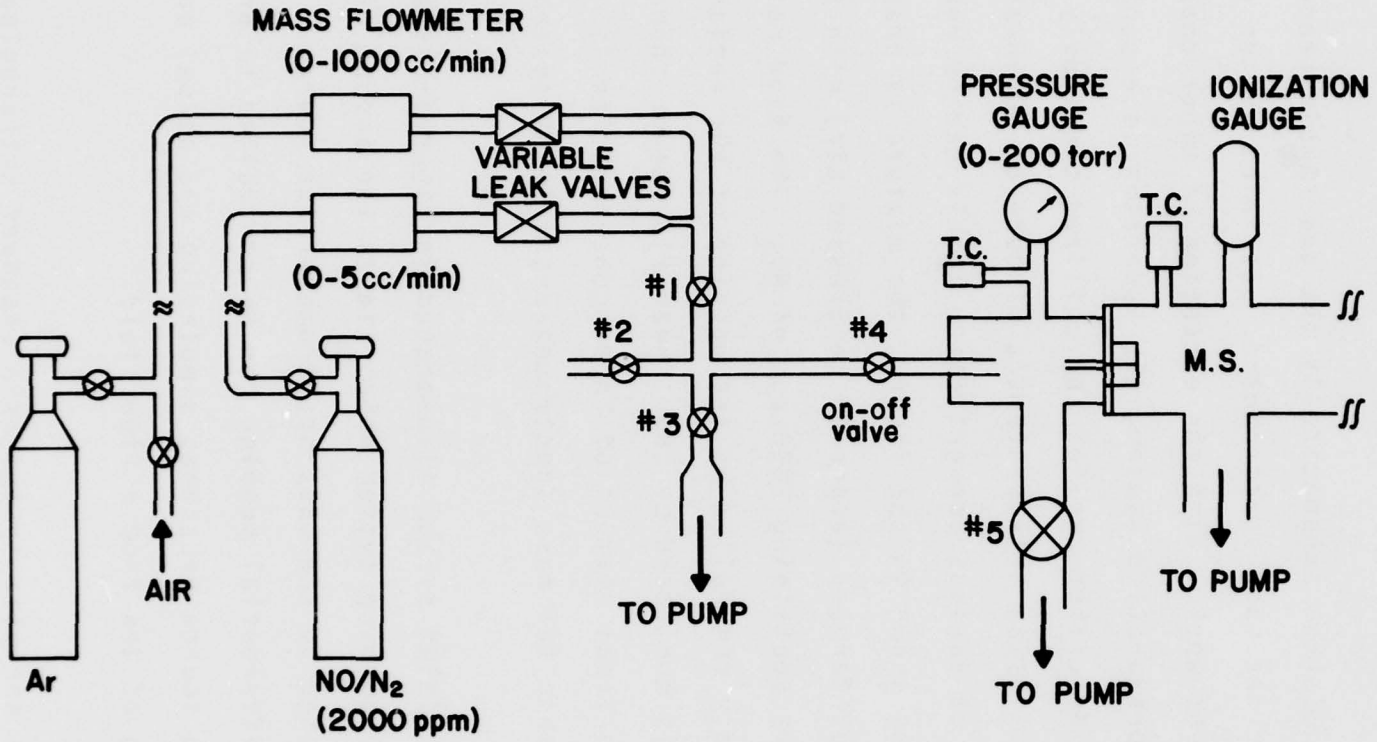

Figure A-1 Schematic Diagram of Sample Preparation and Mass Spectrometric Gas Inlet System

allowing automatic peak switching at any desired rate. Data obtained are recorded on an X-Y recorder, or transmitted to an existing computer system, which in turn reduces the data into desired format. All required calibration of the system has been essentially completed in the course of earlier studies.

RESULT AND DISCUSSION

A. Low Electron Beam Energy Analysis

The only mass spectral peak suitable for monitoring nitric oxide (NO) with a typical mass spectrometer is the NO^+ ion (mass/charge ratio = 30). This ion is the most abundant ion formed from NO upon electron impact at a standard electron beam energy of 70 eV. In the absence of complications, the monitored NO^+ ion intensity, I_{30}, should therefore be directly related to the concentration level of NO present in the gas sample. However, the actual situation is often more complicated in that any component of the sample to be analyzed which yields ions of m/e 30 under electron impact will constitute a positive interference to the measurement of the NO concentration. In a typical case, where NO is to be analyzed in a mixture where air is the major component, an isotope ion ($^{15}N^{15}N^+$) will be formed which also has the same nominal m/e ratio as that of the NO^+ ion. The intensity of this isotope ion is typically larger by an order of magnitude or more than that of the NO^+ ion.

One method of avoiding the above described complication is to minimize the formation of undesirable ions by appropriate selection of electron beam energy. The appearance potential of the NO^+ ion from NO is 9.25 eV. This is the lowest energy required to form this ion by electron impact on NO. In addition,

among the molecules which are potential sources of m/e 30, NO has the lowest ionization potential. In principle then, ionization of interferences can be avoided by operating at an electron energy of 9.25 eV. In practice, however, the sensitivity is quite low at this energy and thus the electron energy is preferably set at some higher value which permits adequate detection capability and still minimizes ionization of interfering compounds.

As an illustration of these methods, a mass spectrum of air containing 10 ppm of NO obtained with the electron beam energy at 12.5 eV, is shown in Figure A-2. A mass spectrum of pure air obtained under identical conditions is shown in Figure A-3. A significantly larger intensity of m/e 30 is observed in Figure A-2,which is due to the formation of the NO^+ ion from NO. From these experiments, it was determined that the lower limit for the detection of NO in air is better than 10 ppm using the method described. More detailed studies must be conducted, based on signal/noise considerations, in order to assess the actual lower limit of detection.

B. High Electron Beam Energy Analysis

As noted above, a major limitation in using a low energy electron beam for the detection of NO at low concentration levels is the relatively poor sensitivity at low energy. This may

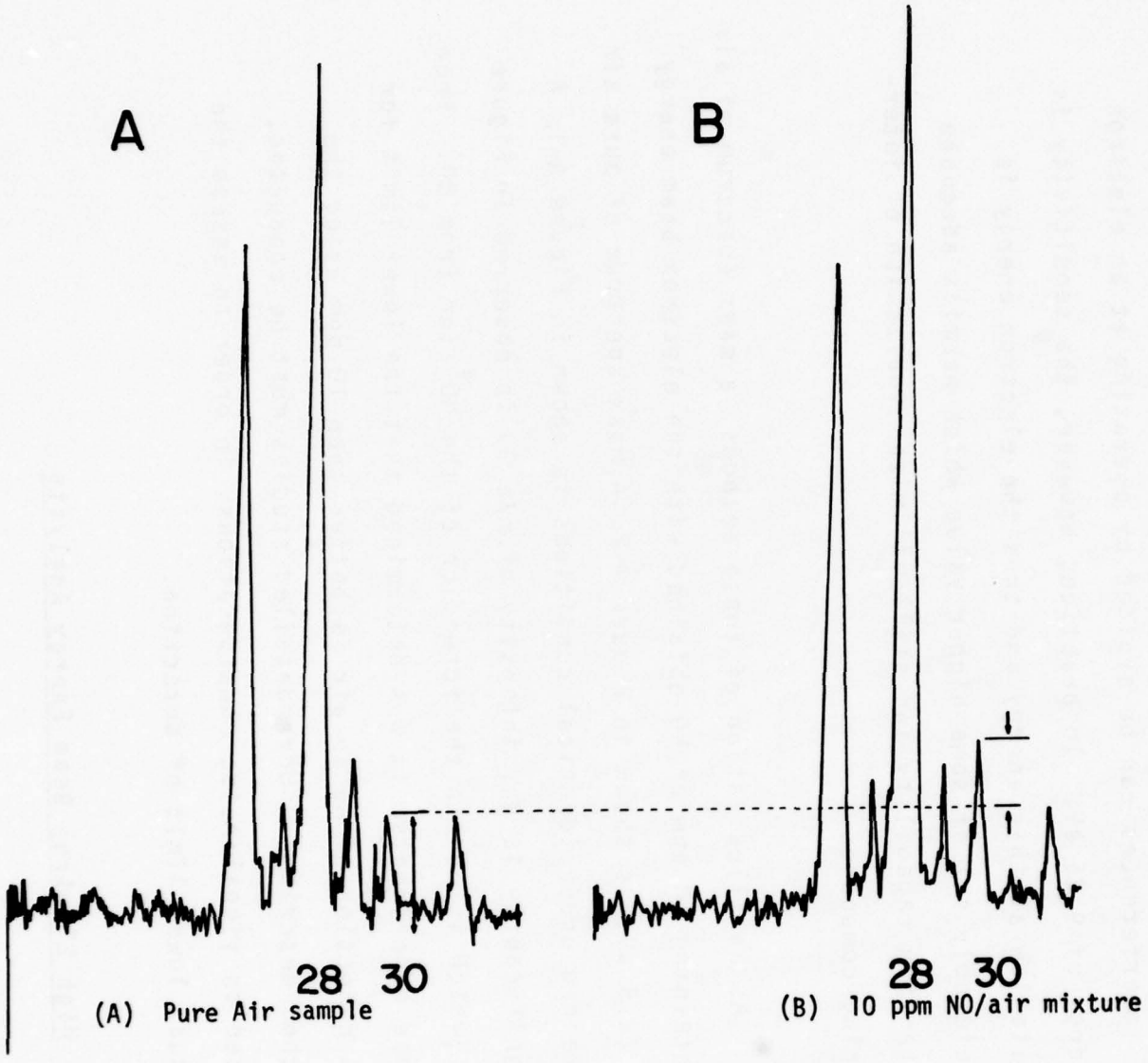

Figure A-2 Mass Spectra of Gas Samples Obtained Using 12.5 eV Electron Ionizing Energy

effectively limit the lowest detectable NO concentration under these conditions to about 10 ppm. At higher electron energies (typically 70 eV), for the same NO source pressure, the absolute intensity of the NO^+ ion is easily increased by two orders of magnitude over that attainable at low electron energy. As already mentioned, however, this increase in the intensity of NO^+ ion is also accompanied by an even sharper increase in the formation of ions such as $^{15}N_2^+$ (also m/e 30), if one is dealing with an NO/air mixture. Again though, this may result only in a relatively constant background signal which can readily be subtracted from the total m/e 30 ion intensity. On the other hand, there may also be present compounds contributing to m/e 30 which vary in concentrations and for which such corrections cannot be accomplished. For example, gases such as nitrous oxide (N_2O) and nitrogen dioxide (NO_2) also yield NO^+ upon electron impact. However, the extent of formation of NO^+ from these compounds is much less than that from nitric oxide, and can be ignored as long as the concentrations of these gases is significantly lower than that of nitric oxide. Interference from hydrocarbons (which form $C_2H_6^+$, also nominal m/e 30), is also negligible (except for ethane), unless the concentrations of these are several orders of magnitude greater than that of nitric oxide.

Under favorable conditions then, it is possible to detect low levels of NO more reliably using a higher energy electron beam.

the data obtained are not sufficiently accurate to warrant further detailed quantita-

Preliminary tests were conducted using this mode of operation with the APL quadrupole mass spectrometer. The results are presented here to illustrate the capability of this procedure. Figure A-4 shows the mass spectrum of the standard 2000 ppm NO/N_2 mixture, while Figure A-3 presents the background spectrum obtained just prior to the introduction of the NO/N_2 mixture. Within the recorded mass range (that is, m/e 25 to m/e 40), the intensities of all ions except m/e 28, 29 and 30 are practically unchanged with the introduction of the mixture gas. Apparently, the increased m/e 28 and m/e 29 ion intensities correspond to the $^{14}N_2^+$ and $^{14}N\ ^{15}N^+$ ions formed from N_2 in the mixture gas. While a portion of the increased m/e 30 component (95%) of it can be attributed to formation of the NO^+ ion, which is indicative of the NO gas in the mixture.

One procedure for monitoring the NO concentration in a mixture involves operation of the mass spectrometer in the specific ion monitoring mode. In this mode, the mass spectrometer is tuned to detect only the ion of interest (in this case the ion of m/e 30) and this ion is continuously monitored and the level is recorded. Any change of NO concentration will immediately cause a change in the monitored ion signal, the extent of the change reflecting variations in the NO concentration.

With the present experimental arrangement, the NO concentration of the prepared NO/air mixture can also be directly

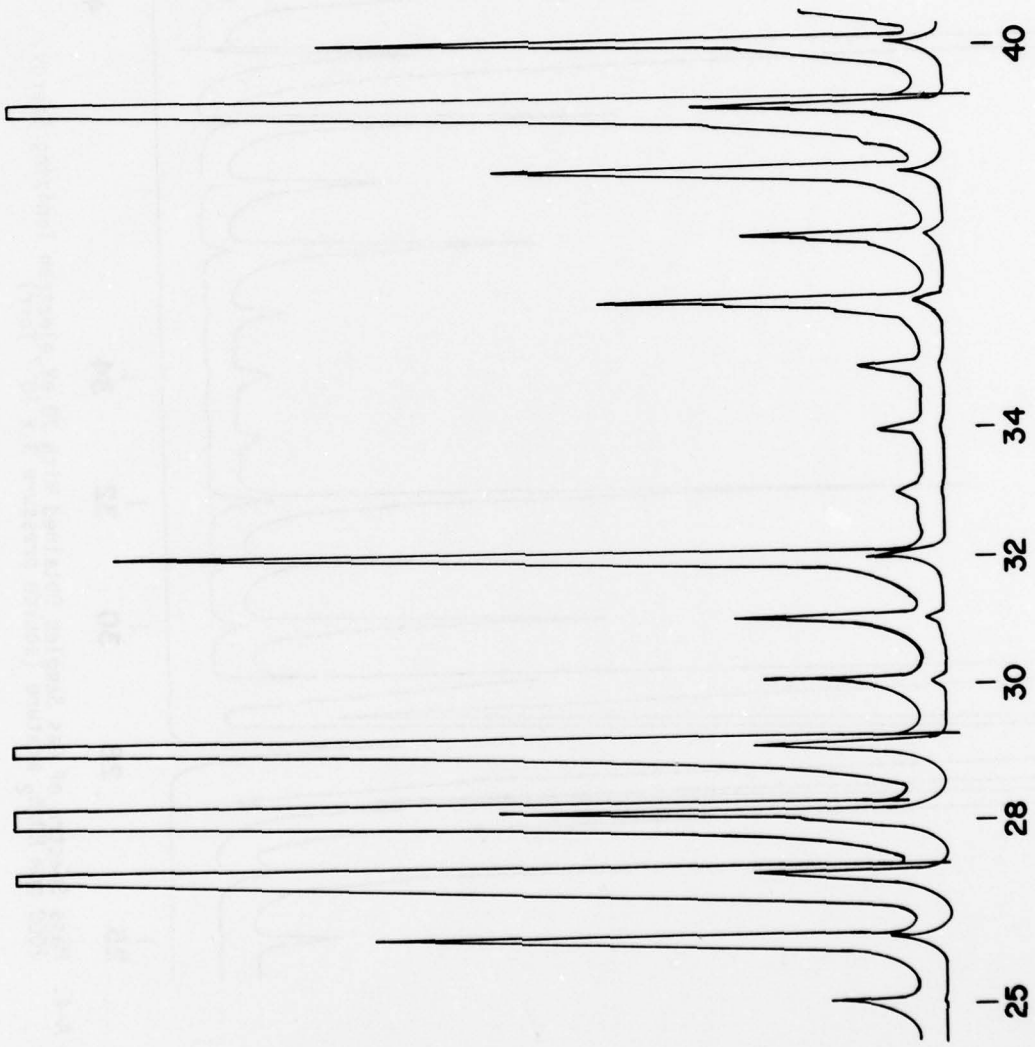

Figure A-3. Mass Spectra of Gas Samples Obtained With 70 eV Electron Ionizing Energy, Background (Source Pressure 0.6×10^{-4} Torr)

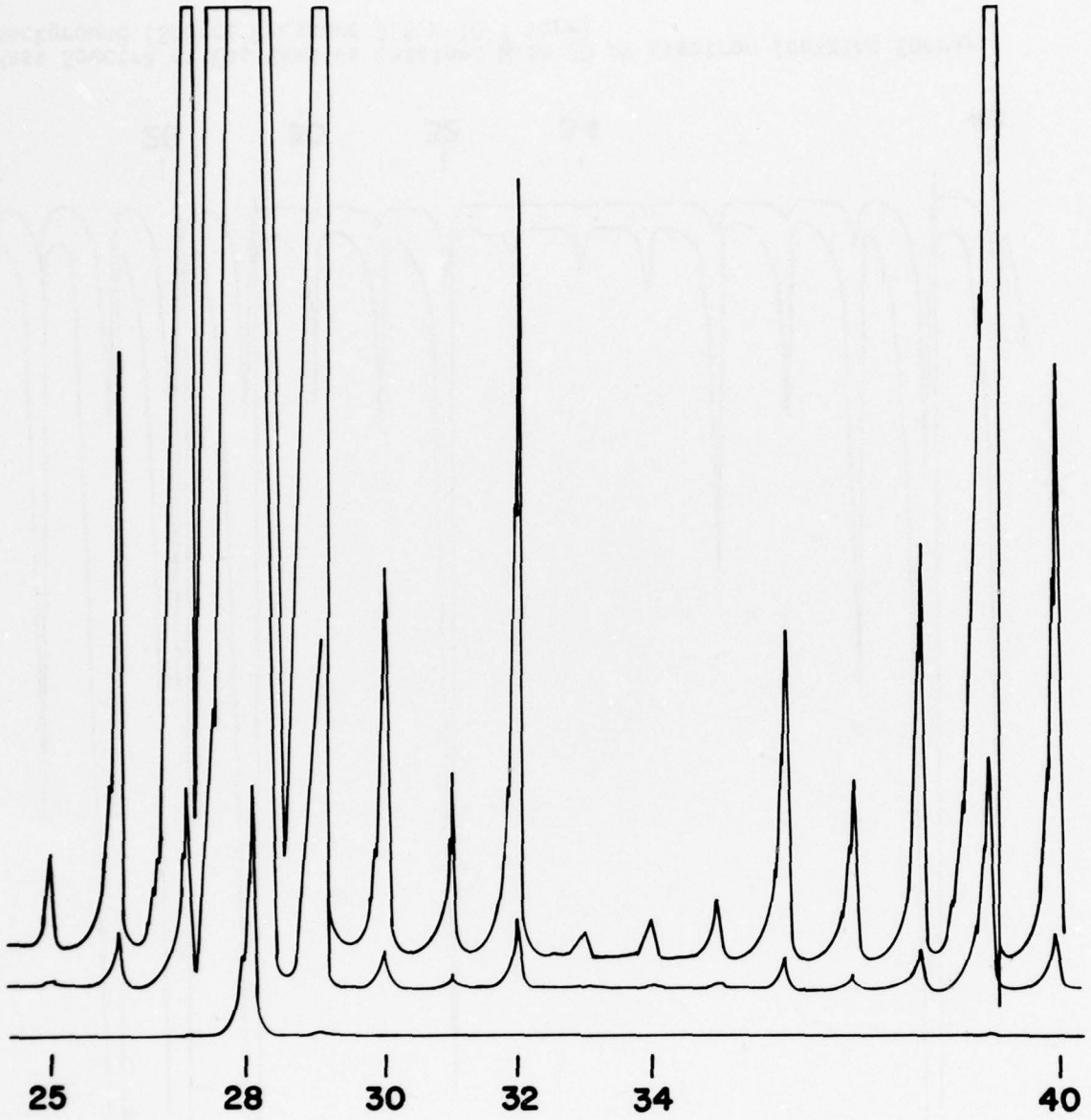

Figure A-4. Mass Spectra of Gas Samples Obtained With 70 eV electron Ionizing Energy, 2000 ppm NO/N_2 mixture (source pressure 3 x 10^{-7} Torr)

monitored from the mass flow rate data. Typically an NO/air mixture is prepared by mixing compressed air, at a fixed flow rate of 500 cc/min, with the standard NO/N_2 mixture (containing 2000 ppm NO), the flow rate of the latter being varied from 0 to 5 cc/min. This yields a final mixture having NO concentrations ranging from 0 to 20 ppm in air. As described in the earlier section, the rate of both gas flows are continuously monitored in these studies by the linear mass flow meters shown in Figure 1. The application of this method is illustrated in Figure 4, which is a plot of the m/e 30 ion signal as a function of the NO concentration in air, obtained directly from the X-Y recorder trace. Here, the x-axis input of the recorder is provided by the voltage output of the flow meter which monitors the flow rate of the standard NO/N_2 mixture. The Y-axis input corresponds to the voltage signal of the mass spectrometer, which is tuned to the ion of m/e 30. In this instance, a substantial fraction of the monitored m/e 30 ion signal was contributed by ions other than the NO^+ ion (such as $^{15}N\ ^{15}N^+$) and part of the signal is also due to background normally recorded in the present system. In Figure 4, this interfering ion signal has been artificially offset in order to provide a clearer indication of the increase of m/e 30 due solely to NO^+ arising from NO in the gas sample. It can be seen in this figure that the monitored m/e 30 ion intensity increases linearly with increasing NO concentration over the entire experimental range. Levels

of NO as low as a few ppm can readily be detected. However, the ultimate detection limit appears to be largely limited by the random noise which is rather large, as seen in Figure A-5. In order to lower the NO detection limit, and improve the accuracy of analysis, a signal averaging method should be utilized.

Figure A-6 is a schematic presentation of the m/e 30 peaks measured by the mass spectrometer both before and after the NO sample was introduced into the mass spectrometer ion source. In the specific ion monitoring mode just described, the heights of the corresponding m/e 30 peaks were actually compared as a quantitative indication of the NO concentration level. A substantial fluctuation in the monitored ion signal will occur if the mass spectrometer "detunes", that is, if a drift in voltage occurs so that the instrument is no longer tuned to the exact center of the mass peak. To avoid fluctuations caused by such drifting, it is desirable to scan the spectrum over a short mass region in the vicinity of the center of the ion peak of interest. The mass spectrometer is provided with an automatic scanning capability for this purpose. This capability, coupled with the existing APL computer system, facilitates ion signal integration, and no major instrument modifications are required.

Several different ion integration methods were tested in the present NO monitoring experiment. The first method entails

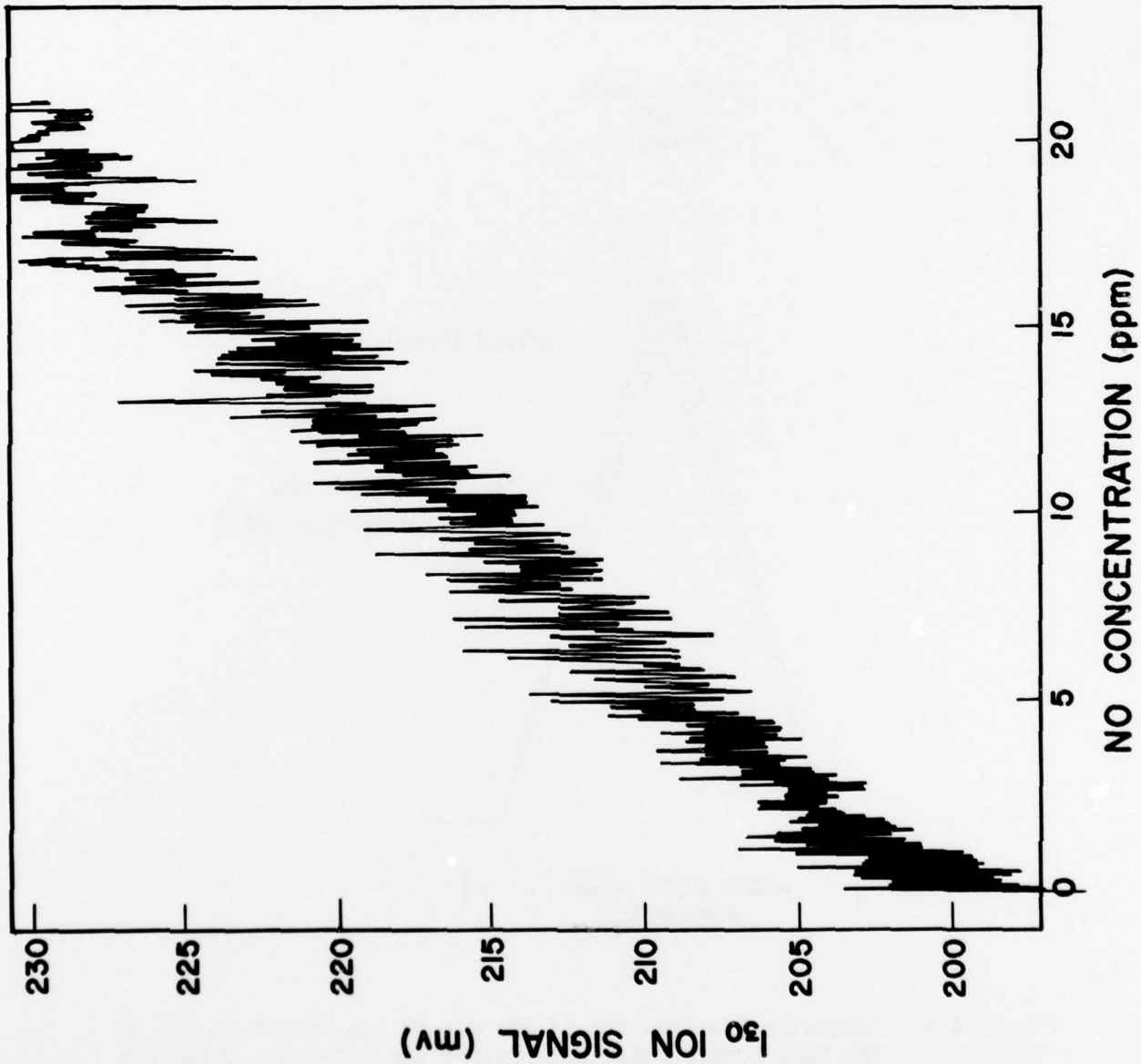

Figure A-5. Recorder Plot of the m/e 30 Signal as a Function of NO Concentration in Air

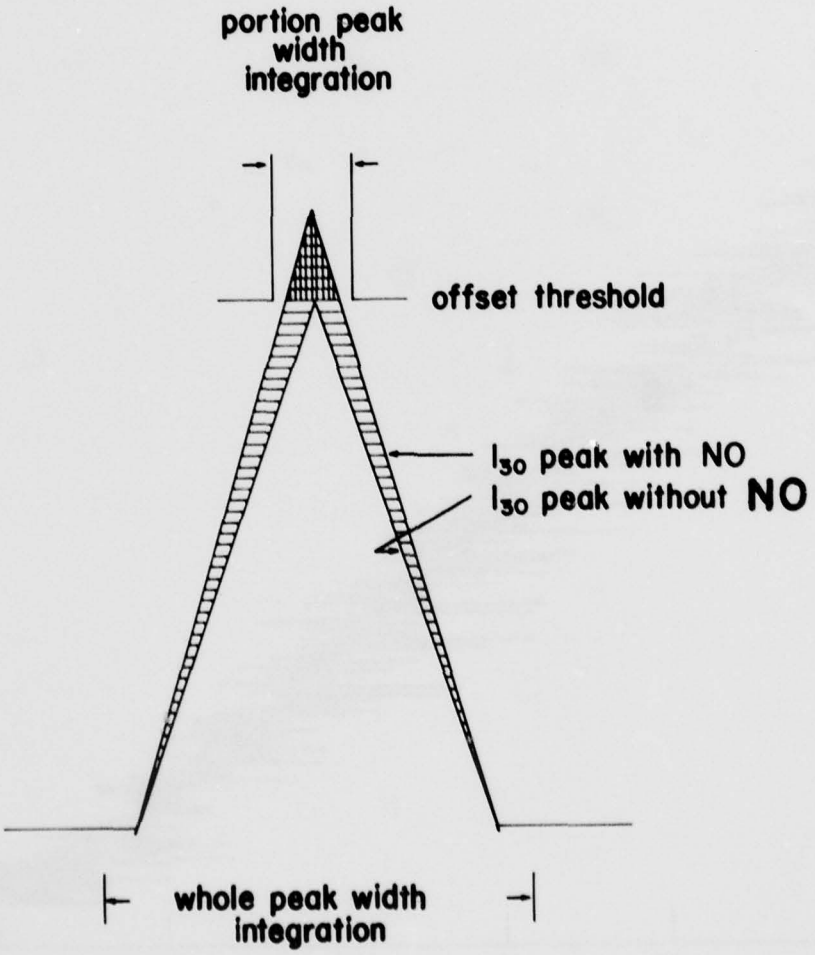

Figure A-6. Schematic Presentation of the m/e 30 Ion Peak Recorded in the Mass Spectrometer Both Before and After the Injection of the Air Stream

integration of only the peak area above a preselected threshold level (the area with the shaded grid in Figure A-6). In theory, this area is most sensitive to the change of NO concentration, since it is mainly contributed by the NO^+ ion, and does not include contributions from other species commonly present in the background. Also, using this mode, the mass spectrometer can be tuned at a more sensitive setting (such as higher electron emission current, higher electron multiplier voltage, etc.) without causing signal saturation at output. Figure A-7 shows the circuit diagram of an added device which allows only the offset ion signal to be transmitted to the computer input.

The result of the integration technique just described is illustrated in Figure A-8, which is a plot of the integrated ion intensity as a function of the NO concentration, ranging from 0-10 ppm, in a NO/argon mixture. A total of ten measurements are obtained at each NO concentration level measured. The results are seen to be highly reproducible over the entire experimental range. The established lowest detection limit is 2 ppm of NO in argon. It appears, however, that the integrated peak area is not linear with respect to the concentration of NO present in the sample. This is apparently an artifact caused by offsetting the ion signal. As seen in Figure A-6 an increase in NO concentration will not only cause a linear increase in the NO^+ signal voltage, but apparently also causes the width of the peak above threshold to be increased somewhat. This results in

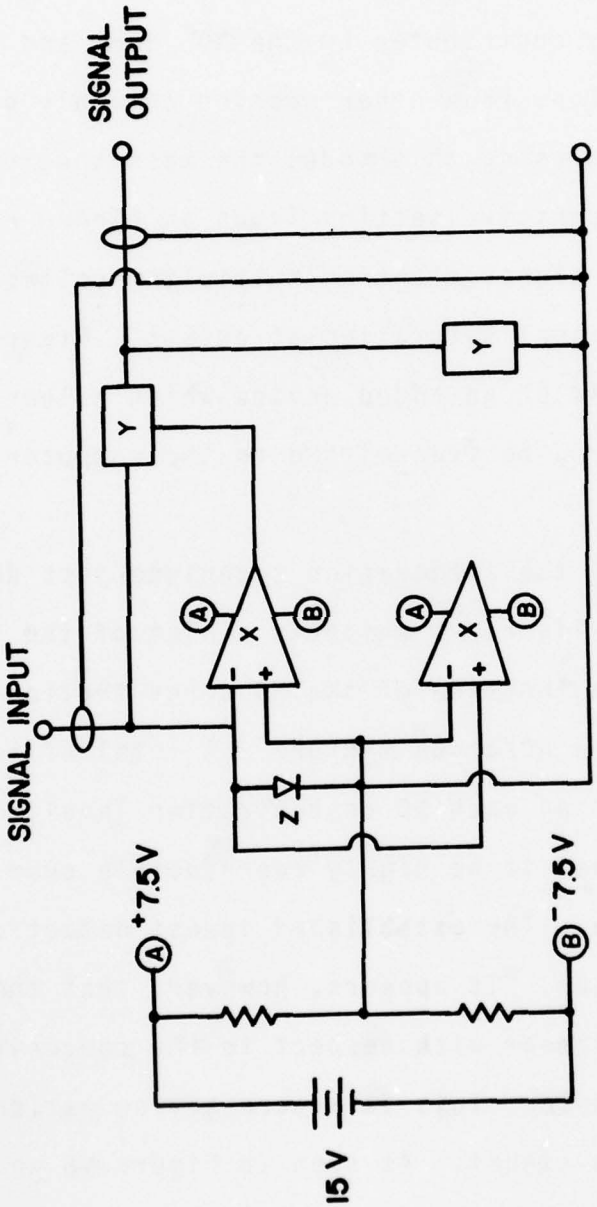

Figure A-7. Circuit Diagram of the Ion Signal Offset Device
X (comparator)
Y (MOS switch)
Z (diode)

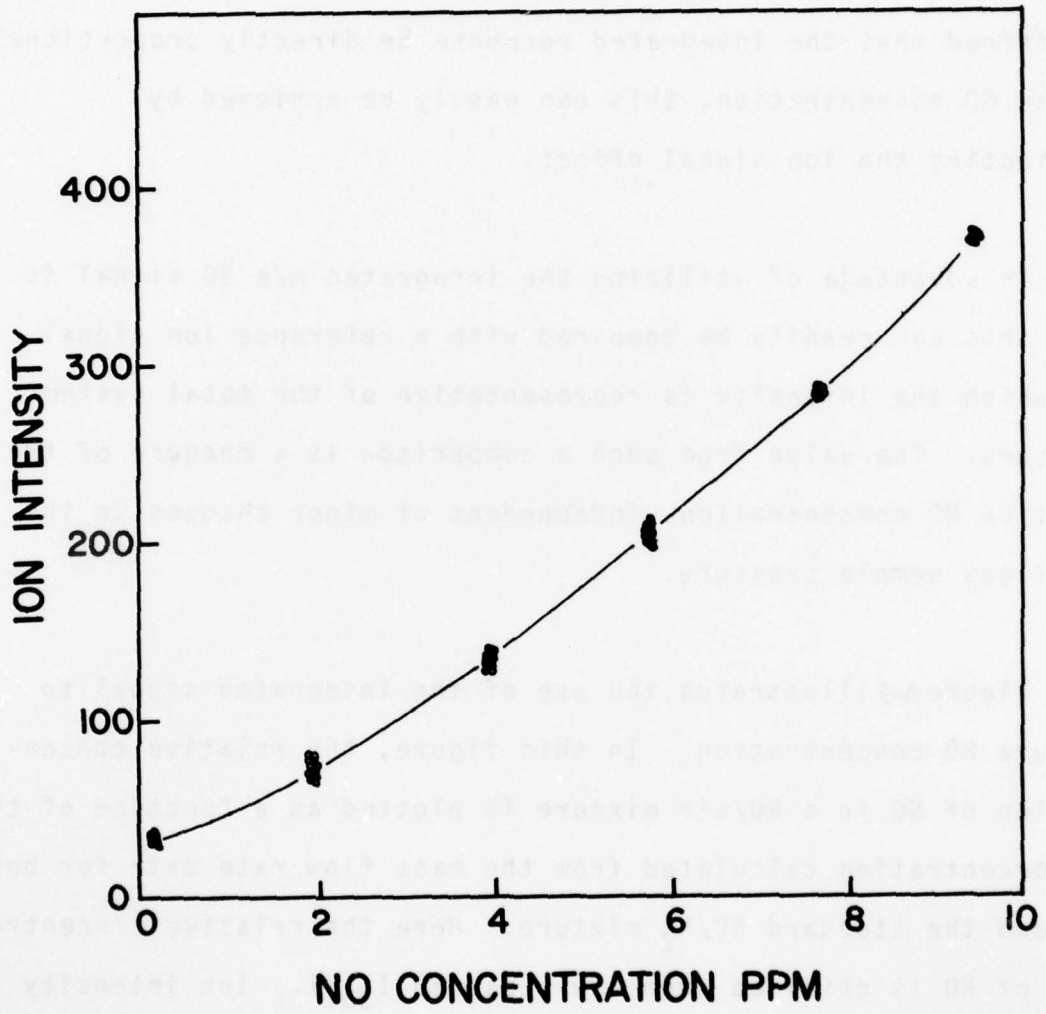

Figure A-8. Plot of Integrated Intensity of I_{30} Above a Preselected Threshold Level vs NO Concentration in the NO-argon Mixture

a non-linear increase in the integrated peak area with increasing NO concentration. In principle, this non-linear response of the integrated signal should not be a problem as long as the data obtained are reproducible, and accurate calibration has been accomplished prior to measurement of an unknown sample. If it is desired that the integrated response be directly proportional to the NO concentration, this can easily be achieved by eliminating the ion signal offset.

An advantage of utilizing the integrated m/e 30 signal is that this can readily be compared with a reference ion signal for which the intensity is representative of the total system pressure. The value from such a comparison is a measure of the relative NO concentration, independent of minor changes in the total gas sample pressure.

Figure A-9 illustrates the use of the integrated signal to measure NO concentration. In this figure, the relative concentration of NO in a NO/air mixture is plotted as a function of the NO concentration calculated from the mass flow rate data for both air and the standard NO/N_2 mixture. Here the relative concentration of NO is obtained from the measured I_{30}/I_{34} ion intensity ratio after correcting for the m/e 30 background. I_{34} is the integrated intensity of the $^{17}O\ ^{17}O^+$ ion which is chosen as a reference ion. The intensity of this ion is comparable to that of m/e 30 within the experimental range used here. This simplifies the computer data reduction. It is seen from Figure 8

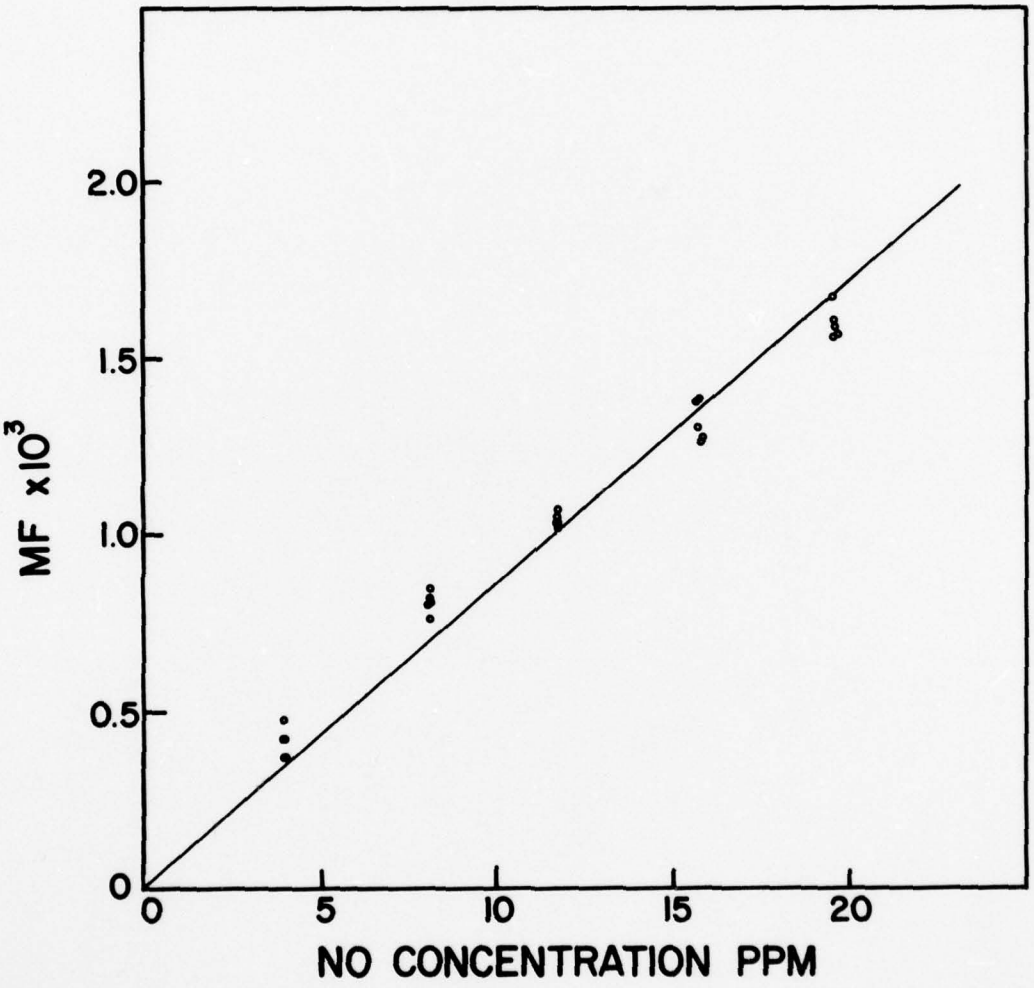

Figure A-9. Plot of Integrates Intensity of I_{30} vs NO Concentration in the NO/Air Mixture

that within the experimental NO concentration range, 0-20 ppm, the measured relative value is linear with respect to the actual NO concentration level. The lowest detection limit established from this plot is 4 ppm of NO in air.

CONCLUSION

The preliminary results presented in this report establish that in-situ measurement of nitric oxide at parts-per-million levels can be achieved with the mass spectrometric analysis system. Detection of NO can be accomplished using either low or high energy electron beams. The choice between these two options depends largely on the nature of interfering compounds in the gas sample to be analyzed.

REFERENCES

1. Chang, C., Sides, G., and Tiernan, T. O., "In-Situ Measurements of Gas Species Concentrations in Simulated Dump Combustor Flow Fields; AFAPL -TR-76-105 Air Force Aero Propulsion Laboratory, November 1976.

2. Drewry, J. E., "Characterization of Sudden-Expansion Dump Combustor Flow Fields," AFAPL-TR-76-52 Air Force Aero Propulsion Laboratory, July 1976; Drewry, J. E., to be published.

☆U.S.Government Printing Office: 1978 — 657-002/307